MASTER OF SCIENCE IN COMPUTER SCIENCE AND ENGINEERING

Enhanced Graph Convolutional Networks for ASD Diagnosis: A Multimodal Transfer Learning Based Approach Using Chebyshev Spectral Graph and Attention Mechanism

Adnan Ferdous Ashrafi
171041014

Department of Computer Science and Engineering
Islamic University of Technology
August, 2025

Enhanced Graph Convolutional Networks for ASD Diagnosis: A Multimodal Transfer Learning Based Approach Using Chebyshev Spectral Graph and Attention Mechanism

Adnan Ferdous Ashrafi
171041014

Department of Computer Science and Engineering
Islamic University of Technology
August, 2025

CERTIFICATE OF APPROVAL

The thesis titled **"Enhanced Graph Convolutional Networks for ASD Diagnosis: A Multimodal Transfer Learning Based Approach Using Chebyshev Spectral Graph and Attention Mechanism"** submitted by Mr. Adnan Ferdous Ashrafi with student ID 171041014 of Academic Year 2017-18 has been found as satisfactory and accepted as partial fulfillment of the requirement for the degree Master of Science in Computer Science and Engineering on August 14, 2025.

Board of Examiners:

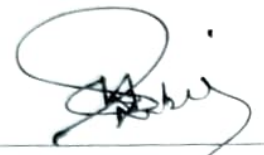

Dr. Md. Hasanul Kabir
Professor
Department of Computer Science and Engineering,
Islamic University of Technology (IUT), Gazipur.

Chairman
(Supervisor)

Dr. Md. Hasanul Kabir
Professor and Head
Department of Computer Science and Engineering,
Islamic University of Technology (IUT), Gazipur.

Member
(Ex-Officio)

Dr. Abu Raihan Mostofa Kamal
Professor
Department of Computer Science and Engineering,
Islamic University of Technology (IUT), Gazipur.

Member
(Internal)

Dr. Hasan Mahmud
Professor
Department of Computer Science and Engineering,
Islamic University of Technology (IUT), Gazipur.

Member
(Internal)

Dr. M. Shamim Kaiser
Professor
Institute of Information Technology (IIT)
Jahangirnagar Univeristy, Savar, Dhaka.

Member
(External)

Declaration of Candidate

This is to certify that the work presented in this thesis is the outcome of the analysis and experiments carried out by Adnan Ferdous Ashrafi under the supervision of Dr. Md. Hasanul Kabir, Professor, Department of Computer Science and Engineering, Islamic University of Technology (IUT), Dhaka, Bangladesh. It is also declared that neither this thesis nor any part of it has been submitted anywhere else for any degree or diploma. Information derived from the published and unpublished work of others have been acknowledged in the text and a list of references is given.

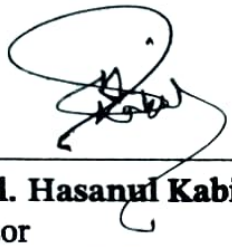

Dr. Md. Hasanul Kabir
Professor
Department of Computer Science and Engineering
Islamic University of Technology (IUT)
Date: August 14, 2025

Adnan Ferdous Ashrafi
Student ID: 171041014
Date: August 14, 2025

Dedicated to my parents, teachers, and the one who made this work possible for their lifelong dedicated support to my efforts.

Contents

List of Figures

List of Tables

List of Abbreviations

ASD	Autism Spectrum Disorder
TD	Typically Developed
CNN	Convolutional Neural Network
GCN	Graph Convolutional Network
fMRI	Functional Magnetic Resonance Imaging
sMRI	Structural Magnetic Resonance Imaging
Phe	Phenotypic Data
GAT	Graph Attention Networks
CDC	Centers for Disease Control and Prevention
ADOS	Autism Diagnostic Observation Schedule
SRS	Social Responsiveness Scale
ADI-R	Autism Diagnostic Interview-Revised
CARS	Childhood Autism Rating Scale
ABIDE	Autism Brain Imaging Data Exchange
ADNI	Alzheimer's Disease Neuroimaging Initiative
PDD-NOS	Pervasive Developmental DisorderNot Otherwise Specified
MMDB	Multi-modal Dyadic Behavior
MSDL	multisubject dictionary learning
SVM	Support Vector Machine
RF	Random Forest
TDA	Topological Data Analysis
AE	Autoencoders
FCN	Fully Connected Network
EV-GCN	Edge variational Graph Convolutional Network
MSE-GCN	multiscale enhanced graph convolutional network
MMGCN	Local Global Multimodal Domain Adaptation
LGMDA	multi-modal graph convolutional network
SACDL	Sparse Adaptive Prior Coupled Dictionary Learning
DRL	deep reinforcement learning
EGCN	Enhanced graph convolutional network
GAN	Generative Adversarial Network
AUC	Area under Curve
NLL	Negative Loss Likelihood
PCP	Preprocessed Connectome Project
CPAC	Configurable Pipeline for the Analysis of Connectomes
EVD	eigenvalue decomposition

Acknowledgement

I would like to express my whole-hearted gratitude to Allah Subhanu Wata'ala for giving me strength to complete this study, and being with me when none was there beside me. I would also like to express my grateful appreciation to Dr. Md. Hasanul Kabir for his constant motivation and support throughout this study. I would also like to express my heartfelt gratitude to the one dearest to me, whose unwavering support remained constant - even through my repeated failures. I would also like to express my gratitude to the people associated with Computer Vision Lab (CVLab).

I would like to express my deepest gratitude to my parents for their unwavering love, support, and encouragement throughout my academic journey. Their sacrifices, patience, and belief in my potential have been the driving force behind my achievements. They have instilled in me the values of hard work, perseverance, and integrity, which have guided me not only in my studies but in every aspect of life. This thesis is as much a reflection of their dedication as it is of my own efforts, and I am forever indebted to them.

Abstract

Autism Spectrum Disorder (ASD) is a complicated neurodevelopmental disorder marked by variation in symptom presentation and neurological underpinnings, making early and objective diagnosis extremely problematic. This paper offers a Graph Convolutional Network (GCN) model, incorporating Chebyshev Spectral Graph Convolution and Graph Attention Networks (GAT), to increase the classification accuracy of ASD utilizing multi-modal neuroimaging and phenotypic data. Alongside, a transfer learning approach has been utilized in separate experiments to explore the possibility of knowledge transfer in GCN based architectures. Leveraging the ABIDE I dataset, which contains resting-state functional MRI (rs-fMRI), structural MRI (sMRI), and phenotypic variables from 870 patients, the model leverages a multi-branch architecture that processes each modality individually before merging them via concatenation. Graph structure is encoded using site-based similarity to generate a population graph, which helps in understanding relationship connections across individuals. Chebyshev polynomial filters provide localized spectral learning with lower computational complexity, whereas GAT layers increase node representations by attention-weighted aggregation of surrounding information. Also, transfer learning leads to a more robust feature generalizations across domains. Extensive trials illustrate the model's superiority, reaching a test accuracy of 74.82% and an AUC of 0.82 on the whole dataset, and a transfer learning based approach achieved an accuracy of 72.89% and an AUC of 0.79, surpassing multiple state-of-the-art baselines, including conventional GCNs, autoencoder-based deep neural networks, and multi-modal CNNs. Ablation studies further demonstrate the incremental influence of each architectural component, emphasizing the usefulness of the methods using graph attention, hyper-parameter adjustment, and transfer learning. The results validate the effectiveness of graph-based deep learning for ASD classification, notably in combining multi-modal data and capturing complicated inter-subject interactions. This work takes a crucial step toward building reliable, scalable, and objective computer-aided diagnostic methods for ASD.

Chapter 1

Introduction

Autism Spectrum Disorder is a complex neurological disease characterized chiefly by deficits in social communication and interaction, alongside repetitive behaviors and limited interests. The term "spectrum" denotes the extensive range of challenges and strengths exhibited by each individual with ASD. The variability in symptom presentation, in terms of both intensity and type, has rendered ASD a particularly intricate illness to identify and diagnose, particularly during early developmental phases.

Recent surveillance by the U.S. Centers for Disease Control and Prevention (CDC) indicates that Autism Spectrum Disorder affects roughly 1 in 31 children [57], underscoring its increasing prevalence and the pressing necessity for early and accurate diagnostic instruments [42]. Early diagnosis is crucial as prompt intervention, especially during the initial stages of neurodevelopment, has demonstrated a substantial enhancement in language development, cognitive capacity, and adaptive behavior [79].

Historically, ASD diagnosis has depended on expert-administered behavioral exams and organized interviews. Instruments such as the Autism Diagnostic Observation Schedule (ADOS) [39], the Autism Diagnostic Interview-Revised (ADI-R) [40], and the Childhood Autism Rating Scale (CARS) [12] represent the prevailing gold standard. These approaches are inherently subjective, reliant on the clinician's expertise, and necessitate prolonged observation or interview periods, frequently lasting several hours. This approach is not only time-intensive and costly but also sensitive to inter-rater variability and cultural biases [37].

Consequently, there is an increasing interest in enhancing behavioral evaluations with objective, data-driven methodologies that utilize biological indicators.

Magnetic resonance imaging (MRI), encompassing structural MRI and functional MRI (fMRI), has developed as a non-invasive technique that can elucidate neuroanatomical and functional abnormalities linked to ASD [19], [61]. With improvements in machine learning and deep learning technology, researchers now have the possibility to build computer models that can mine patterns from complicated, high-dimensional imaging and phenotypic data. These advances herald a new era of precision diagnostics, presenting hope for earlier, more accurate, and scalable detection of ASD.

1.1 Problem Statement

Despite substantial progress in neuroimaging and computational methods, ASD diagnosis remains a formidable challenge due to multiple unresolved issues at the clinical and technological levels. The current diagnostic process is primarily symptom-based, relying on structured observation and parent/caregiver interviews. Instruments such as the ADI-R, which consists of nearly 100 questions and takes up to 3 hours to administer, are labor-intensive and require specialized clinical expertise [40]. The reliance on caregiver reports also introduces recall biases and socio-cultural subjectivity, which can distort diagnostic accuracy [13].

The emergence of neuroimaging as a diagnostic aid has sparked considerable interest in developing biologically-informed diagnostic markers. Structural MRI has revealed anomalies in brain regions including the amygdala, corpus callosum, and cerebellum in individuals with ASD, while functional MRI has indicated alterations in resting-state connectivity across the default mode and salience networks [66]. However, these findings are inconsistent and often vary between studies, partly due to limited sample sizes, cohort heterogeneity, and inter-site variability.

From a machine learning standpoint, traditional classification methods using imaging data are limited in their capacity to integrate multi-modal signals and often fail to account for the networked nature of brain organization. Most approaches utilize voxel-based or region-based features in isolation, neglecting the interactions between regions - critical for understanding ASDs complex neural underpinnings. Additionally, the inherent heterogeneity of ASDspanning genetic, neurobiological, and phenotypic dimensions - complicates model training and leads to poor generalization.

Also, traditional approaches do not account for the fusion of information or features from a multimodal perspective. Thus, there seems to be a gap in information passing

from higher levels of the architecture towards the classification layer. Furthermore, no reliable transfer learning approach is present, and thus, this domain remains unexplored.

1.2 Motivation and Research Scopes

The motivation for this research is grounded in the urgent societal and clinical need for a more reliable, scalable, and objective ASD diagnostic framework. Delayed or missed diagnoses can result in children not receiving timely interventions, exacerbating long-term cognitive, educational, and social impairments. Current reliance on clinical observation and interviews does not scale well across different regions or populations, particularly in low-resource settings where access to expert clinicians may be limited.

Neuroimaging offers a pathway to objective diagnostics, but its full potential remains underutilized due to analytical limitations. There is a need to move beyond static feature-based representations of brain images and towards models that capture complex, multi-dimensional interactions. This necessitates a multi-modal fusion frameworkwhere imaging data, phenotypic metadata, and even genetic profiles can be jointly considered to reflect the multi-factorial nature of ASD.

Graph neural networks (GNNs), especially GCNs [76], have shown substantial promise in capturing higher-order relationships in brain networks. By treating each individual as a node in a graph with associated features (e.g., MRI-based regional metrics) and connecting them based on phenotypic similarity or connectivity profiles, GCNs allow for group-level learning while respecting individual-level variability. This graph-based modeling framework provides a more holistic and personalized representation of neurobiological data.

The objectives of this research is therefore centered on:

- Building an end-to-end GCN-based framework that integrates structural and functional MRI data with phenotypic information.l
- Mitigating inter-site variability through domain adaptation and normalization techniques
- Validating the proposed model using standard dataset(s) to ensure robustness and generalizability
- Integrate and deploy attention networks to impose importance on parts that are

much more responsible than others

- Apply transfer learning techniques to enable knowledge transfer from pre-trained model weights

1.3 Research Challenges

The detection and classification of ASD using neuroimaging and machine learning are fraught with a range of methodological, biological, and computational challenges:

1. **Biological and Clinical Heterogeneity**: ASD presents differently across individuals, with a wide range of cognitive and behavioral profiles. This heterogeneity is mirrored in neuroimaging findings, where no single biomarker has achieved clinical utility [19]. Sub-types within ASD may differ significantly in terms of brain structure, connectivity, and response to treatment.

2. **Data Quality and Inter-Site Variability**: Large-scale datasets like the Autism Brain Imaging Data Exchange (ABIDE) [44] have been pivotal in ASD research. However, ABIDEs multi-site nature introduces significant variation due to differences in scanner types, image resolution, and acquisition protocols. These factors lead to site-specific biases that challenge model generalizability.

3. **Small Sample Sizes and High Dimensionality**: Neuroimaging data is inherently high-dimensional, and often, the number of subjects is much smaller than the number of features, making models prone to over fitting [67]. This is exacerbated when incorporating multi-modal data, which increases complexity.

4. **Integration of Multi-modal Data**: While the fusion of imaging and non-imaging data can improve classification performance, integrating these diverse modalities is complex. Imaging features are continuous and spatial, while phenotypic data can be categorical or ordinal. Effective fusion strategies are essential to preserve the integrity of each modalitys contribution.

5. **Model Interpretability**: Deep learning models, including GCNs, are often criticized for their lack of transparency. Clinical deployment demands not only accuracy but also interpretability - understanding why a model makes a specific prediction is critical for trust and adoption in healthcare settings [16].

6. **Application of transfer learning**: The use of transfer learning to diagnose brain disorders is still largely unexplored, despite encouraging developments in addressing data scarcity in medical imaging. The diversity of brain illnesses, such as Alzheimer's disease (AD) and autism spectrum disorder, presents a significant obstacle since, despite having some neuropathological characteristics in common, they show different connection patterns and clinical presentations. In order to avoid negative transfer, it is necessary to carefully align structural and functional representations when transferring knowledge across such domains. Furthermore, the direct reuse of learnt features across tasks is made more difficult by the high-dimensionality and noise inherent in brain network data. The absence of defined standards for assessing transferability between neuroimaging datasets, such ABIDE and ADNI [35], is another drawback, especially when taking demographic diversity and variations in acquisition techniques into account. Therefore, creating transfer learning frameworks that can preserve task-specific subtleties, take advantage of shared biomarkers, and choose transferable components intelligently is still an important and unexplored research area. Improving the generality, robustness, and interpretability of transferable models in clinical contexts should be the main goal of future research.

1.4 Research Contribution

This thesis provides a comprehensive and scalable paradigm for ASD diagnosis that utilizes breakthroughs in graph neural networks and multi-modal data integration. The key research contributions include:

1. **Multi-Modal Graph Construction Framework**: An innovative approach to creating population graphs that integrates imaging data with non-imaging phenotypic attributes. Graph edges are created using a hybrid similarity measure that integrates neuroimaging-derived connectivity and demographic/clinical data.
2. **End-to-End GCN Architecture for ASD Classification**: Development of an upgraded GCN model that contains several convolution layers, attention mechanisms, and residual connections to capture both local and global brain connectivity patterns. The model is meant to conduct node-level classification (i.e., ASD vs. TD) with high accuracy and resilience.
3. **Application of Graph Attention Networks**: Introduction of Graph

Attention Networks, dilated input has enabled the model to capture robust and multi-faceted features. Techniques graph attention, residual networks and dilated input features.

4. **Application of Transfer Learning in Graph Convolutional Networks:** A new and mainly untapped area of study is the incorporation of transfer learning into Graph Convolutional Networks (GCNs) for brain network analysis. Although GCNs have demonstrated impressive ability in graph-structured data modeling, the lack of labeled medical data sometimes limits their usefulness, especially in research on neurological disorders. For the first time, this work shows that transfer learning may be successfully applied to GCNs in the context of classifying brain disorders, particularly across related domains like Alzheimer's disease (AD) and autism spectrum disorder. Even with minimal training data, the method enhances classification accuracy and model generalization by transferring learned representations from a source disorder to a target disease. The outcomes demonstrate notable gains in accuracy and resilience over conventional GCN models trained from scratch, and they are empirically confirmed on benchmark datasets (such as ABIDE I and ADNI). This study offers up new possibilities for utilizing inter-disease correlations to help clinical diagnosis and neuroimaging-based biomarker development, while also highlighting the unrealized potential of merging GCNs with transfer learning.

5. **Extensive Evaluation and Benchmarking**: Validation of the suggested approach on large-scale, multi-site datasets such as ABIDE-I. Comparisons are made with state-of-the-art techniques, focusing on GCN variations.

1.5 Thesis Outline

This document is organized as follows:

Chapter 1 provides an overview of the ASD diagnostic landscape, outlines the research problems, and summarizes key contributions. Chapter 2 reviews existing literature on behavioral diagnostic tools, neuroimaging biomarkers, and computational approaches including machine learning, deep learning, and graph neural networks. In Chapter 3 a detailed description of the data pre-processing pipeline, graph construction strategy, and the architecture of the proposed GCN model is available. Details on feature extraction, graph representation, and training procedures are provided. Chapter 4 presents the experimental setup, including

datasets, evaluation metrics, and bench-marking results. Performance comparisons with baseline models and ablation studies are included. Chapter 5 analyzes results in depth, discusses strengths and limitations of the proposed model, and explores implications for clinical application. Chapter 6 summarizes findings, discusses broader impacts, and suggests future research directions such as longitudinal studies, real-time diagnostics, and integration with genetic data.

Chapter 2

Related Works

The implementation of computer-aided approaches in Autism Spectrum Disorder diagnosis has altered the landscape of neurodevelopmental assessment by offering data-driven, objective, and scalable methodologies to augment traditional clinical examinations. These methods make use of developments in medical imaging, machine learning, and computational neuroscience to examine intricate patterns in phenotypic profiles, behavioral data, and neuroimaging (including structural and functional MRI). At their core, computer-aided diagnostic (CAD) systems strive to uncover biomarkers and predictive features that can help early and reliable detection of ASD, an illness noted for its clinical variability and subtle neurobiological symptoms. Since machine learning, deep learning, and topological data analysis have been integrated, the field has rapidly advanced, with each contributing distinct strengths in pattern recognition, spatiotemporal modeling, and structure discovery. Early implementations concentrated on feature engineering and statistical modeling. Importantly, these methods provide the ability to shorten diagnostic delays, enhance decision-making in under-resourced clinical settings, and promote tailored therapies by quantifying ASD-related neuroanatomical and functional abnormalities. Notwithstanding persistent obstacles like data variability, interpretability, and model generalizability, computer-aided methods are paving the way for a more accurate, repeatable, and biologically informed method of diagnosing ASD, revolutionizing the way researchers and clinicians think about and identify the condition.

2.1 Types of ASD

The complex neurodevelopmental disorder known as Autism Spectrum Disorder is characterized by limited, repetitive patterns of behavior, interests, or activities along with ongoing challenges with social communication and engagement. ASD has historically encompassed several subtypes [20], including Pervasive Developmental Disorder-Not Otherwise Specified (PDD-NOS) [21], Autism Disorder, Asperger's Syndrome, and Childhood Disintegrative Disorder. Nevertheless, as there is increasing agreement that these disorders differ in severity and manifestation but share fundamental neurobiological and behavioral characteristics, these subcategories were combined into a single diagnostic entity, Autism Spectrum Disorder, with the release of the DSM-5 in 2013 [21]. The transition from a category to a dimensional classification underlines the spectrum character of ASD, where individuals may vary greatly in cognitive capacity, linguistic competence, sensory responsiveness, and adaptive functioning. For instance, some individuals with ASD may be minimally verbal with associated intellectual disability, whereas others may possess average or above-average intelligence and fluent language, yet demonstrate substantial challenges in social reciprocity and flexibility [38]. The existence of discrete neurobiological subtypes within the spectrum may be represented by variations in brain connectivity, cortical development, or synaptic function, according to recent attempts at phenotypic clustering and data-driven subtyping, which are frequently backed by neuroimaging and genetic analyses [30], [36]. The necessity of stratified models in clinical practice and computational research is highlighted by this developing understanding, which has significant ramifications for prognosis, tailored therapies, and biomarker discovery.

2.2 Data Modalities in ASD Detection

Autism Spectrum Disorder detection relies on a variety of neurobiological and behavioral data modalities that provide complementary insights into the atypical development associated with the condition. Among these, neuroimaging plays a pivotal role, with structural magnetic resonance imaging (sMRI) and resting-state functional MRI being the most extensively used modalities in computational ASD research. sMRI provides high-resolution anatomical information, enabling analysis of brain volume, cortical thickness, and surface morphology - measures that have been associated with neuroanatomical deviations in ASD, particularly in the frontal, temporal, and cerebellar regions [19]. In contrast, rs-fMRI captures spontaneous

brain activity by measuring blood oxygenation level-dependent (BOLD) signals, allowing the inference of functional connectivity patterns among brain regions; disruptions in default mode, salience, and social cognition networks have been consistently observed in ASD populations [44], [66]. Diffusion tensor imaging (DTI), although less frequently used, offers insights into white matter integrity and structural connectivity, and has revealed abnormalities in corpus callosum and association tracts in individuals with ASD [65]. Beyond neuroimaging, phenotypic and behavioral data - such as demographic profiles, Autism Diagnostic Observation Schedule (ADOS) scores, and Social Responsiveness Scale (SRS) scores - are commonly integrated into machine learning pipelines to enhance classification performance and enable multi-modal analysis [7]. Recent advances have also seen the incorporation of electroencephalography (EEG) and eye-tracking data, which provide temporal precision and behavioral correlates respectively, though their availability is limited in large-scale public datasets. The Autism Brain Imaging Data Exchange initiative, especially ABIDE I, has been instrumental in facilitating multi-modal research by providing harmonized neuroimaging and phenotypic data across multiple sites [44], allowing researchers to explore modality-specific and integrative biomarkers. As ASD is inherently multifaceted, the integration of diverse data modalities holds promise for improving diagnostic precision and uncovering latent sub-types within the spectrum.

2.3 Dataset

Prominent among these is the Autism Brain Imaging Data Exchange program [44], which aggregates comprehensive functional and structural brain imaging data (MRI/fMRI) from individuals with and without ASD across many studies. The Autism Spectrum Disorder detection dataset [78] comprises video clips of "reach-to-grasp" behaviors executed by children both with and without ASD. The DE-ENIGMA [53] dataset provides a comprehensive, multi-modal compilation (audio, video, depth) of interactions among autistic children, accompanied by expert annotations for emotional valence, arousal, auditory characteristics, and bodily movements. The Multi-modal Dyadic Behavior (MMDB) [51] collection comprises multi-modal recordings (video, audio, physiological) and annotations of social and communicative behaviors shown by young children during semi-structured play interactions. The Saliency4ASD dataset [25] offers eye movement data from children with ASD and normally developing individuals as they see diverse pictures for visual attention modeling. The Self-stimulatory behavior dataset [26] was assembled from

public recordings (e.g., YouTube) to classify distinct stereotyped behaviors such as arm flapping, head pounding, and spinning, documented in natural environments. Previous studies have utilized subsets of broader human action recognition, facial expression, and gesture recognition databases when data specific to ASD was scarce. Among all available datasets, ABIDE remains the most potent and clinically accurate depiction of the problem domain.

2.4 Classical Machine Learning Approaches

The use of traditional machine learning algorithms in the identification of Autism Spectrum Disorder has been a pivotal advancement in creating objective, data-driven diagnostic instruments in neuro-developmental research. Initial studies concentrated on utilizing structured features obtained from neuroimaging techniques - specifically functional connectivity matrices from rs-fMRI and volumetric metrics from structural MRI - to identify distinctive patterns linked to ASD. Algorithms such as Support Vector Machines (SVM), Random Forests (RF), and Logistic Regression are extensively utilized for their interpretability, computational efficiency, and resilience in small to medium-sized datasets [6]. These models enhanced comprehension of discriminative brain regions and connection abnormalities, notably within fronto-temporal and default mode networks, which are often associated with ASD. Significantly, conventional machine learning techniques have permitted researchers to investigate model generalizability across multi-site datasets, exemplified by the Autism Brain Imaging Data Exchange (ABIDE I) dataset. The intrinsic variety of ASD symptoms and site-specific variability frequently result in low prediction efficacy, underscoring both the advantages and constraints of traditional machine learning methodologies in elucidating the intricate neurobiological foundations of ASD. Nevertheless, their contributions are essential for establishing baselines, guiding feature selection procedures, and providing interpretable benchmarks for assessing more intricate models like deep neural networks.

2.4.1 Functional Connectivity with SVM / Ridge / Random Forest classifier

Multi-subject dictionary learning (MSDL) was employed by Abraham et al. [3] to derive functional connectivity features, tangentspace embedding, and an L2-regularized SVM classifier as shown in Figure 2.1. In this work, the researchers

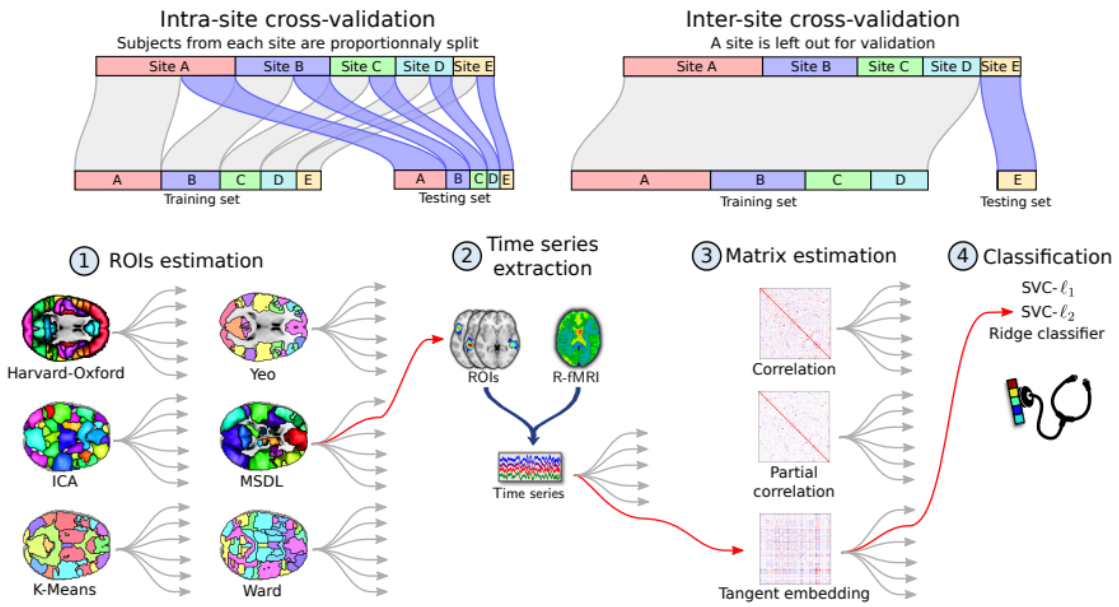

Figure 2.1: Functional MRI analysis pipeline [3]

highlight that SVM yields sensitivity/specificity ≈ 70-75% but performance declines with larger, heterogeneous ABIDE samples. Achieved ≈ 67% accuracy across ≈ 1,000 subjects using multi-site ABIDE I and II datasets.

2.4.2 Structural MRI with Feature Engineering

One major study on structural MRI pre-processing using segmented gray matter area of the brain [52] was reported to use a high-dimensional normalization method known as DARTEL [5]. The images were modulated using the non-linear component during normalization. Furthermore, several studies [45] examining volumetric measures across ABIDE I highlight group differences and pre-processing considerations [52], although classification accuracy using SVM or RF tends to remain modest (≈ 65-70%).

2.5 Topological Data Analysis (TDA) Hybrid Approaches

A new approach to the identification of Autism Spectrum Disorder is provided by Topological Data Analysis (TDA) [43], a potent mathematical framework that has recently come to light for revealing hidden geometric and topological features in high-dimensional data. In contrast to traditional approaches that depend primarily on statistical or spatial correlations, TDA focuses on the structure of data - capturing

aspects such as connectedness, loops, and voids that persist across various scales. TDA allows for the derivation of persistent topological fingerprints that may represent underlying changes in the architecture of the brain networks linked to ASD when combined with neuroimaging data, particularly resting-state fMRI and structural MRI. Even in situations where traditional techniques are insufficient, hybrid models that combine TDA-derived features (such as persistence diagrams, persistence images, and bar-codes) with traditional machine learning algorithms like support vector machines or random forests have shown promise in distinguishing people with ASD from those who are typically developing. These techniques offer resistance to noise and inter-site heterogeneity, making them particularly suited for evaluating diverse datasets like ABIDE I. Moreover, TDA provides interpretable summaries of data complexity and connectivity [77], potentially revealing higher-order organizational disruptions in ASD that are not captured by purely statistical models. Although it is still in its infancy, the incorporation of TDA into the pipeline for detecting ASD has the potential to improve biomarker identification and deepen our comprehension of neuro-developmental disorders from a primarily geometric perspective.

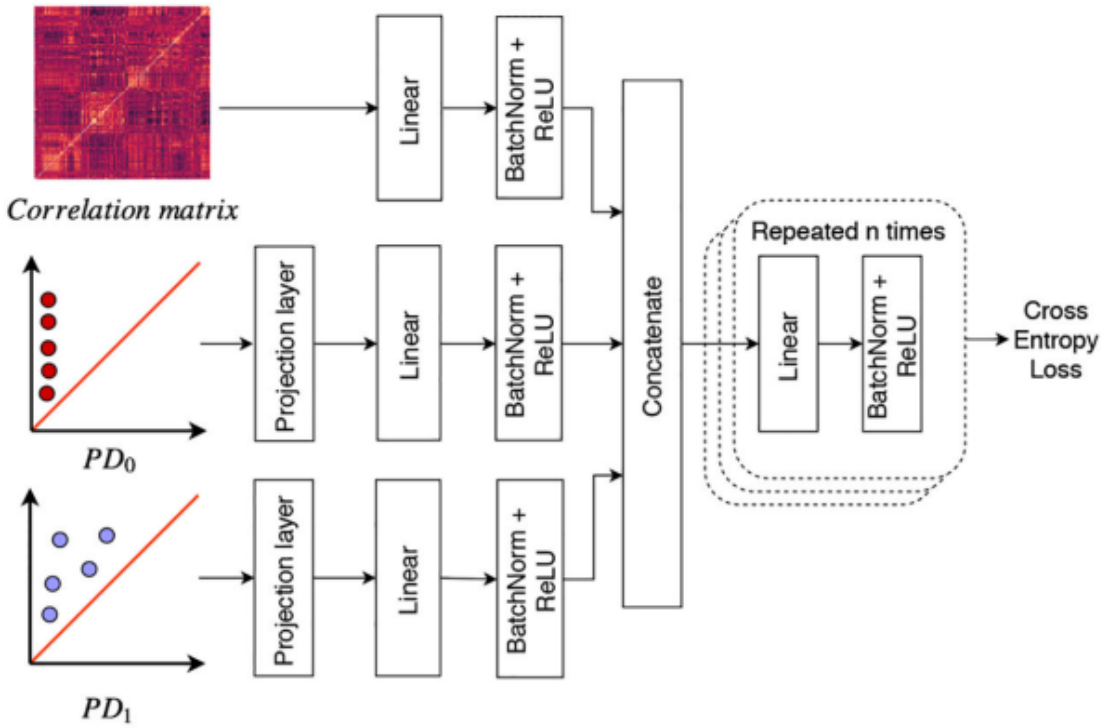

Figure 2.2: Neural Network combining topological features and correlation [50]

2.5.1 Topological Persistence Features with ML Classifier

A study by Rathore et. al [50] combined persistent homology features - persistence diagrams, landscapes, and persistence images - with functional correlation matrices via SVM, random forest, and small neural networks. The proposed architecture is depicted using Figure 2.2. In this work, the authors achieved ≈69.2% accuracy, only a modest improvement over correlations alone. The reported results were not always statistically significant.

2.6 Deep Learning Based systems

Deep learning (DL) has emerged as a revolutionary method for detecting Autism Spectrum Disorder, providing unparalleled ability to model the intricate, high-dimensional, and nonlinear patterns seen in neuroimaging data [72]. In contrast to traditional machine learning techniques that depend on manually crafted features and domain-specific pre-processing, deep learning models like convolutional neural networks (CNNs), recurrent neural networks (RNNs), autoencoders, and graph neural networks (GNNs) [70] can autonomously derive hierarchical feature representations from raw or minimally processed data. This is particularly helpful in ASD research, where impairments in brain structure and function may be subtle, regionally diffuse, and temporally dynamic. Leveraging large-scale, multi-site datasets like ABIDE I, DL models have exhibited promising classification performance by learning from spatial patterns in structural MRI [63] and temporal dynamics in resting-state fMRI [11]. Moreover, recent advancements in hybrid architectures - combining CNNs with long short-term memory (LSTM) networks [62] or attention mechanisms [56] - have enabled deeper exploration of spatiotemporal dependencies relevant to ASD. While challenges such as data scarcity, inter-site variability, and lack of interpretability remain, deep learning continues to push the boundaries of ASD detection by uncovering latent neurobiological features that may elude traditional analytical methods. As such, DL-based techniques are not only boosting diagnosis accuracy but are also giving new possibilities for uncovering clinically meaningful biomarkers.

2.6.1 Autoencoders

One of the first and most notable works in the field of ASD detection was proposed by Heinsfeld et al. [29], where they utilized deep neural networks combining stacked denoising autoencoders and a fully connected network (FCN) on fMRI data from the

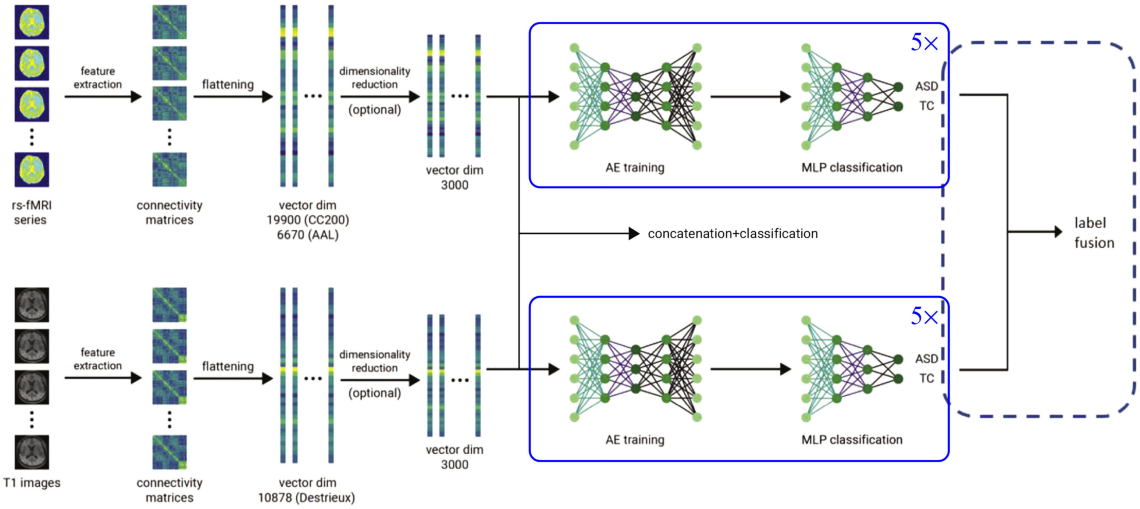

Figure 2.3: Representing of the data classification pipeline using Autoencoder and FCNs [49]

ABIDE dataset, achieving a 70% classification accuracy. Later, building on this, Rakić et al. [49] employed an autoencoder followed by a fully connected network (AE-FCN) along with Ensembles of Multiple Models and Architectures (EMMA), incorporating both functional MRI (fMRI) and structural MRI data as shown in Figure 2.3 to reach a considerable accuracy.

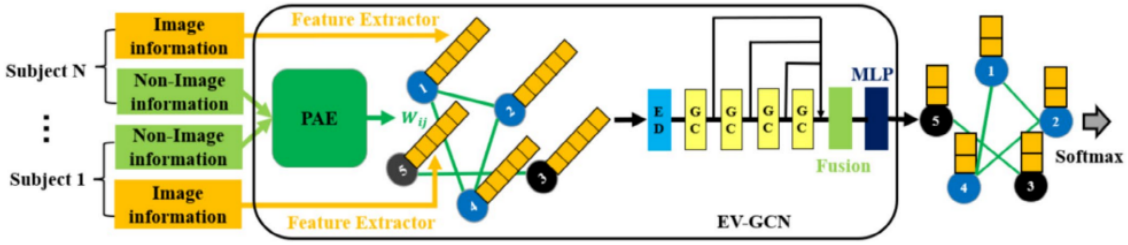

Figure 2.4: The structure of Edge variational GCN [31]

2.6.2 GCN

A graph convolutional neural network (GCN) was first introduced by Parisot et al. [47] that integrates phenotypic information, obtaining a best accuracy of 70.4% on ABIDE fMRI data. Building on the GCN, Huang et al. [31] proposed an edge-variational graph convolutional neural network (EV-GCN), as shown in Figure 2.4, which reportedly achieved 81% classification accuracy. Furthermore, Dong et. al. implemented GCN and Ensemble GCN [15] on the ABIDE I dataset, obtaining 68.6% and 71.3% accuracy, respectively. Song et. al. [59] introduced multi-modal GCN (MMGCN). Here, the authors used a weight-learning network and pairwise associations, deploying multimodal data from the ABIDE I dataset and

obtained an accuracy of 72.37%. A weight-learning deep GCN, as proposed by Wang et. al [69], deployed pairwise associations of non-imaging data into the already existing DeepGCN classification model. The authors achieved an accuracy of 77.27% on a partial testing dataset. Later, Rajaprakash et. al. used the Fuzzy MSE-GCN [48] framework for ASD detection that integrates imaging and non-imaging phenotypic data into a population graph. It uses a fuzzy inference system to calculate graph edge weights based on phenotypic similarity and processes the graph using a multiscale enhanced graph convolutional network (MSE-GCN) with a random walk method. This approach achieved an accuracy of 87% on the ABIDE dataset.

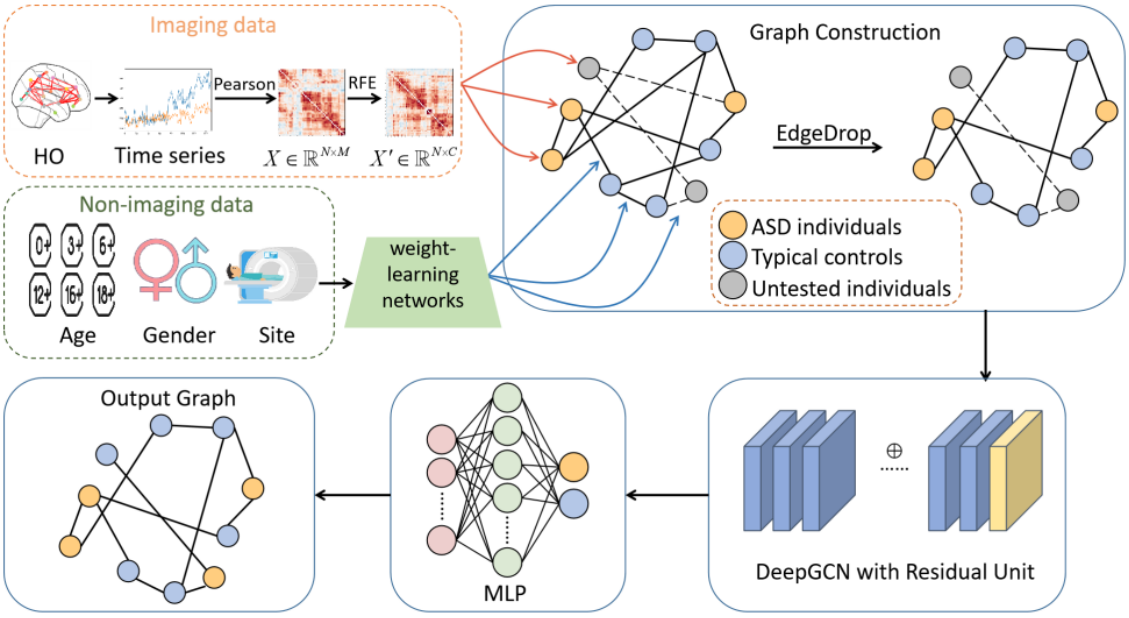

Figure 2.5: Weight Learning DeepGCN architecture [59]

2.6.3 Domain Adaptation

The first use of structural MRI FreeSurfer [22] features across ABIDE I multi-site data were harmonized by Saponaro et. al [54]. After that, Random Forest classification was used as the classifier layer, which improved AUC from ≈0.58 before to ≈0.67 after harmonization. Agestratified results ranged ≈0.620.69. Building on these ideas, Campo et. al. [10] applied adversarial learning to harmonize crosssite functional connectivity features, improving crosssite generalizability on ABIDE I and II datasets in classification tasks.

Local Global Multimodal Domain Adaptation (LGMDA) paired with Sparse Adaptive Prior Coupled Dictionary Learning (SACDL) framework [74] employs LGMDA to perform multi-source domain adaptation and SACDL for sparse-adaptive

coupled dictionary learning to fuse sMRI (regional morphology) and fMRI (functional connectivity) features. The approach enhances ASD classification performance on the ABIDE dataset, achieving an accuracy of 75.32%.

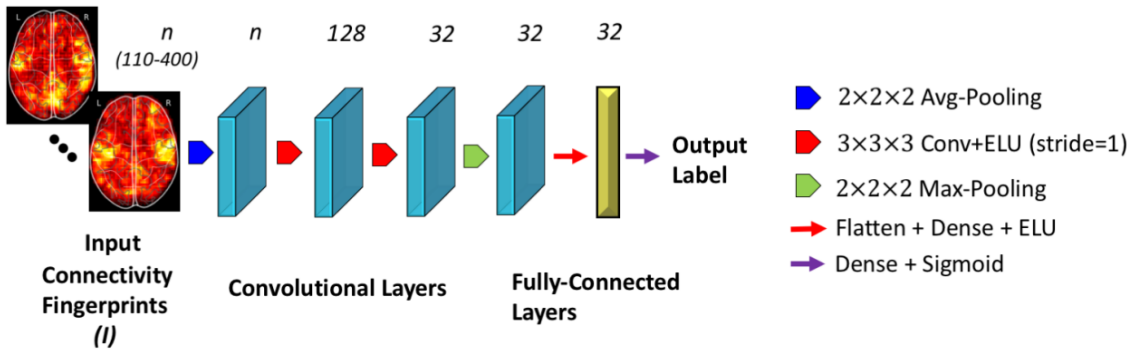

Figure 2.6: The 3DCNN architecture for 3D fMRI ASD classification [34]

2.6.4 Convolutional Neural Network Based Systems

One of the first works based on the application of CNNs in ASD detection was proposed by Khosla et al. [34], and they used volumetric 3DCNNs as shown in Figure 2.6 that operate on fullresolution 3D fMRI volumes rather than ROI summaries. The model was trained on $N > 2000$ ABIDE samples. Later on, Abbas et al. deployed DeepMNF [1], a multi-modal CNN on the ABIDE I dataset, and obtained an accuracy of 75.14% on a partial testing set. The authors utilized both sMRI and fMRI data available from the dataset. Saponaro et al. utilized a multi-modal deep learning model employing a joint fusion approach [55] that was developed by integrating harmonized structural and functional MRI data. Feature representations were learned by feature-reduction neural networks for each modality and combined by a classification neural network, with prediction loss back-propagated to enhance feature learning. This approach achieved an accuracy of 85% $\pm$0.12 and AUC of 0.78 $\pm$0.04 on a partial testing dataset, and is highlighted as the first study to utilize a joint fusion approach.

2.6.5 FCN and ViT based Systems

Building on previous ideas, Jain et. al [32] alleged use of DenseNet201 and MobileNetV2 CNNs trained on functional connectivity heat-maps stratified by age groups (6-11, 11-18, 6-18 years). The best accuracy in this work achieved was $\approx$72.2% for the youngest group.

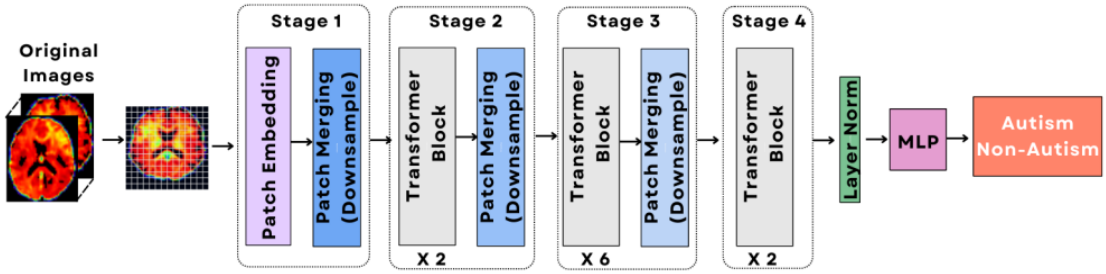

Figure 2.7: TinyViT for ASD classification [24]

Much later, Gupta et al. [24] deployed TinyViT as present in 2.7 to exploit the generalizability of transfer learning using a student-teacher network on the ABIDE I dataset. The authors achieved an accuracy of 76.62% on a partial testing dataset. Du et al. [17] deployed a fully connected network (FCN) based system as the preliminary classifier to achieve an accuracy of 68.98% on the testing dataset.

2.6.6 SpatioTemporal Models: CNN paired with LSTM

A hybrid 3DCNN along with a 3DConvLSTM architecture to model 4D spatiotemporal fMRI data was introduced by ElGazzar et al. [23]. Evaluated on singlesite ABIDE I (NYU, UM subsets), achieving F1 scores of ≈0.78 and ≈0.70, respectively.

2.6.7 Other Deep Architectures: RNN, Autoencoders, GAN augmentation

Building on existing ideas of application of deep learning in ASD detection, Bayram et al. [8] applied RNNLSTM to ROI timeseries on ABIDE I (403 ASD, 468 HC), obtaining≈74.7% accuracy and ≈72.9% sensitivity. Later, Almuqhim et al. [4] used a stacked autoencoder (SAE) on ABIDE I (505 ASD, 530 HC), reaching ≈70.8% accuracy and ≈62.2% sensitivity. Shrivastava et al. [58] used a classic CNN on rs-fMRI ROI-based connectivity, yielding ≈82.7% accuracy, ≈88% sensitivity/specificity on ABIDE I (505 ASD, 530 HC).

2.6.8 Reinforcement Learning Classifier

Exploring recent reinforcement learning techniques, Stember et al. [60] proposed a deep reinforcement learning (DRL) approach trained on graphlabel pairs (functional connectivity) from ABIDE I. DRL outperformed supervised deep models significantly, with F1 score ≈76 vs 67 for standard DL.

2.6.9 Generative Adversarial Networks for Data Augmentation

Later a method using GANs was used by Khan et al. [33] to synthesize additional fMRI data per site (augmenting each to 100 ASD/100 TD), then a parallel CNN + GAN classification pipeline. Applied to ABIDE I, claimed increased robustness across 16 sites (≈3200 total after augmentation).

2.7 Transfer Learning Based Approach

TE-HI-GCN was presented by Li et al. [35], a novel framework that uses functional brain networks derived from fMRI to investigate transfer learning inside GCNs for the diagnosis of brain disorders. This groundbreaking work represents a major advancement in the field of neuro-informatics by applying transfer learning to GCNs across two related but different neurological conditions: Alzheimer's disease (AD) and Autism Spectrum Disorder.

In order to ensure that only significant topological information is transferred and to prevent negative transfer, the transfer learning is meticulously carried out at various graph sparsity levels. According to experiments, the transfer strategy increases classification accuracy, which is crucial for medical applications, particularly in low-data regimes.

The authors achieved an accuracy of 58.30% and an AUC of 0.57 on the ABIDE I dataset.

2.8 Recent Advances in Chebyshev-based Spectral GNNs

Recent advances show that Chebyshev polynomial filters remain central in spectral graph neural networks (GNNs). ChebNet [14] introduced truncated Chebyshev expansions to approximate Laplacian spectral filters efficiently, later simplified to first-order GCNs. However, instability from unconstrained coefficients limited performance. ChebNetII [28] addressed this by reformulating coefficient learning via interpolation, achieving scalability to billion-edge graphs and renewed state-of-the-art results. In parallel, newer variants adopt alternative polynomial basessuch as Bernstein polynomials [27] to improve stability, capture mid and high-frequency information, and adapt to heterophilous graphs [73].

These stabilized spectral GNNs are now applied widely: in spatio-temporal

forecasting (e.g., STGCN and successors for traffic), neuroscience (EEG/fMRI graph decoding), molecular property prediction, and physics/point-cloud modeling. Across domains, the key theme is that basis choice and coefficient constraints govern stability and expressivity. Consequently, modern architectures frequently pair Chebyshev-style spectral filters with temporal modules, attention, or hierarchical pooling, confirming their versatility for both homophilous and heterophilous settings.

2.9 Summary

The detection of Autism Spectrum Disorder has evolved significantly through the integration of diverse computational approaches, ranging from classical machine learning to advanced deep learning and hybrid techniques. Traditional models such as support vector machines and random forests have offered foundational insights but often suffer from limited generalizability due to their reliance on handcrafted features. Topological Data Analysis has introduced a geometric perspective by capturing persistent structural patterns, offering marginal yet interpretable improvements. Deep learning methods, particularly autoencoders, 3D convolutional neural networks, and graph convolutional networks, have demonstrated superior performance by learning hierarchical representations from neuroimaging and phenotypic data. Among these, multi-modal GCNs and ensemble CNNs consistently outperform others in classification accuracy, especially when trained on harmonized, multi-site datasets. Domain adaptation techniques further enhance generalization by addressing inter-site variability, while spatiotemporal models capture dynamic brain activity patterns more effectively. The incorporation of attention mechanisms and transformer-based architectures reflects a shift toward more expressive models capable of handling complex data structures. Additionally, generative models such as GANs have been employed for data augmentation, mitigating class imbalance, and improving model robustness. Collectively, these advancements underscore a growing emphasis on multimodal integration, scalability, and interpretability in the pursuit of reliable computer-aided ASD diagnostics.

Chapter 3

Proposed Approach

For this study, a multi-modal neural Graph Convolutional Neural network architecture, along with transfer-learning based approach has been adopted for classification tasks, specifically tailored to integrate different types of brain imaging and phenotypic data. The architecture employs graph convolutional layers alongside an attention mechanism to leverage both feature information and graph structural relationships. The experimentation also utilizes the transfer learning approach to transfer knowledge from a pre-trained model. The complete pipeline of the proposed model is illustrated in Figure 3.1.

3.1 Research Methodology

In this research, we want to explore the capabilities of graph-based deep learning methods for ASD classification. In order to do that, we need to represent the multi-modal data using population graphs. We also want to explore the application of a transfer learning approach along with a GCN to further enhance the learning process. The overall methodology can be visualized in 3.1. Finally, we also like to deploy specialized methods of deep learning techniques to ensure proper generalization in the problem domain. The overall process is as follows:

- Data Acquisition
  - Feature Engineering
  - Feature Extraction
- Proposed model
  - Multi-Branch GCN architecture

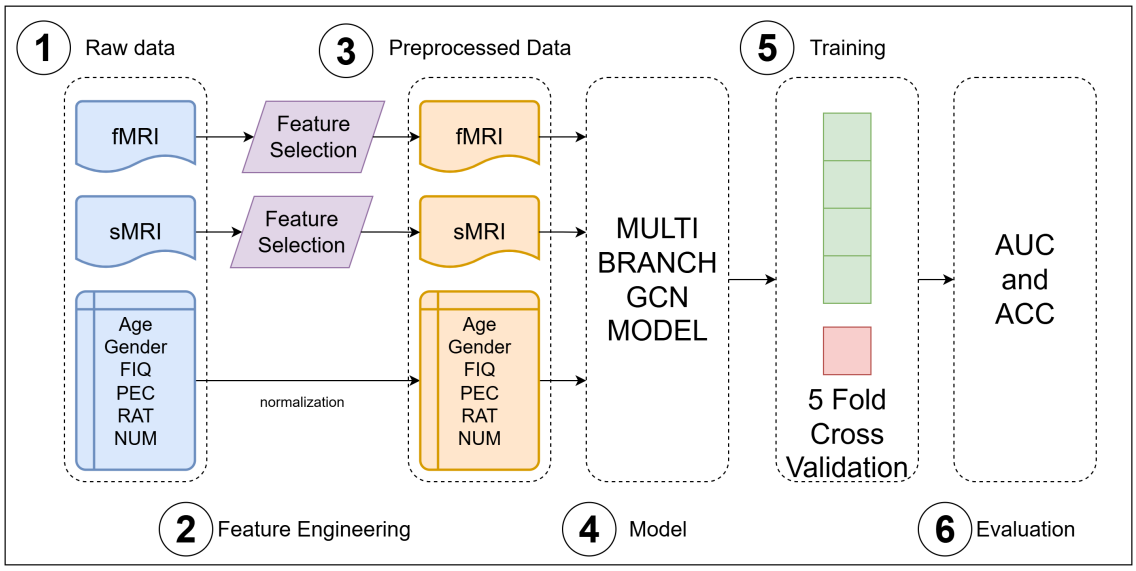

Figure 3.1: Overview of the research methodology

  - Transfer Learning Based Multi-Branch GCN architecture

- Model Training
  - Hyper-parameter tuning
  - Validation evaluation
- Evaluation
  - Accuracy
  - Area Under Curve (AUC)

3.2 Dataset Acquisition

The ABIDE dataset is a significant, open-access neuroimaging collection aimed at enhancing the comprehension of Autism Spectrum Disorder by extensive brain imaging analysis. It contains data from over 1,100 individuals, including both ASD cases and normally developing controls, gathered across 20+ international sites. The dataset comprises resting-state functional MRI and structural MRI images, plus phenotypic information such as age, sex, IQ, and diagnostic scores (e.g., ADOS, ADI-R). ABIDE provides cross-site harmonization and is frequently used for deep learning-based categorization, brain connection studies, and functional network modeling. The dataset is separated into ABIDE I and ABIDE II, with ABIDE II enhancing subject variety and improving phenotypic coverage.

Table 3.1: Sample Distribution in ABIDE I Dataset

Site	Total	ASD	TD
NYU	184	79	105
UCLA	111	52	59
KKI	109	52	57
OHSU	104	52	52
Michigan	79	36	43
Trinity	75	23	52
Pitt	61	29	32
Yale	56	28	28
Caltech	21	10	11
Leuven_1	27	15	12
Leuven_2	27	14	13
MaxMun	26	14	12
SDSU	28	14	14
Stanford	35	19	16
USM	75	58	17
CMU	23	13	10
Brown	25	10	15
Total	**1,112**	**539**	**573**

3.2.1 Preprocessed Connectome Project

To ease repeatable and uniform analysis of ABIDE data, the Preprocessed Connectome Project (PCP) [9] offers a collection of preprocessed rs-fMRI datasets utilizing many common workflows. These include C-PAC, NIAK, AFNI, and FSL, delivering outputs such as functional connectivity matrices, parcellated time series, and voxel-wise characteristics. The initiative provides uniformity in preprocessing steps like motion correction, spatial normalization, nuisance regression, and smoothing, making the ABIDE dataset more accessible to researchers unfamiliar with raw neuroimaging data. The PCP effort has dramatically advanced ASD research by enabling plug-and-play usage of ABIDE for deep learning, machine learning, and statistical modeling.

3.2.2 Dataset Description

The ABIDE I dataset comprises a total of 1,112 subjects, including 539 individuals diagnosed with Autism Spectrum Disorder and 573 typically developing controls, collected from 20 international sites as shown in Table 3.1. Participants range in age from 6 to 64 years, with a mean age of approximately 17.4 years. The dataset exhibits a strong male predominance, with about 88% male and 12% female subjects. ABIDE I provides two primary neuroimaging modalities: resting-state functional MRI and

high-resolution T1-weighted structural MRI. To facilitate reproducible and standardized analyses, preprocessed versions of the dataset are made available through the Preprocessed Connectome Project (PCP), using pipelines such as C-PAC, NIAK, and others.

3.3 Data Preprocessing

A critical instrument for the preliminary preprocessing of resting-state functional magnetic resonance imaging (rs-fMRI) data is the Configurable Pipeline for the Analysis of Connectomes (CPAC). The CPAC was specifically applied to the ABIDE-I dataset in the context of this study. In order to guarantee the data's comparability and integrity, the pipeline includes critical procedures such as spatial normalization, artifact elimination, and motion correction. Its primary function is to effectively standardize the data and resolve challenges associated with inter-site variability prior to the execution of subsequent high-level computational analyses. After processing with CPAC, the study encountered issues with missing time series data, which required the removal of incomplete data to maintain quality. This resulted in a final ABIDE-I dataset of 408 Autism Spectrum Disorder patients and 468 healthy control (HC) individuals, despite its utility.

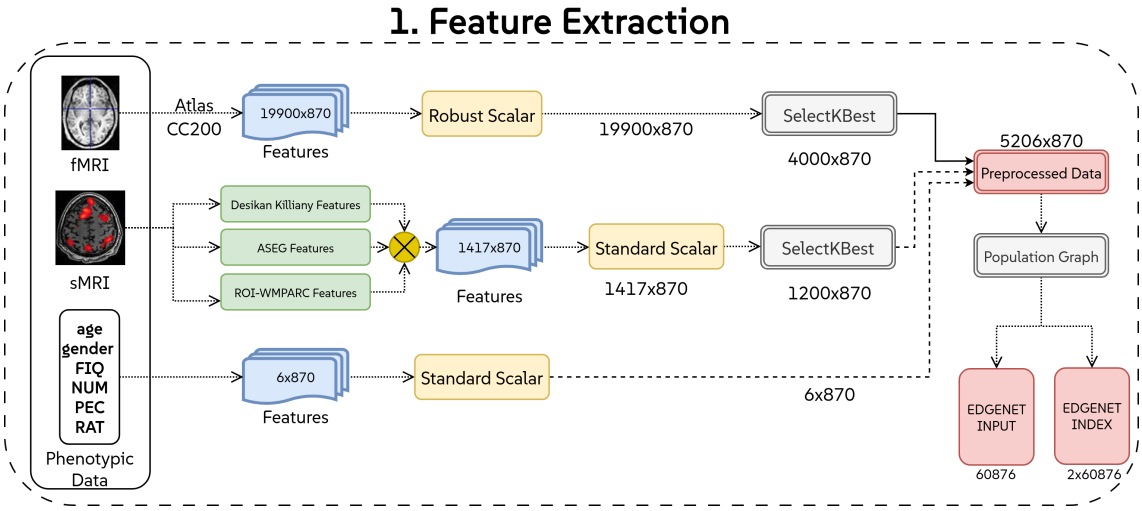

Figure 3.2: Feature extraction process for the proposed pipeline

3.4 Chebyshev Spectral Graph Convolution

The Chebyshev Spectral Graph Convolution layer [14], a fundamental element of the proposed graph Convolutional Neural Network (CNN) framework, makes substantial contributions to the generalization of CNNs to irregular domains such as graphs. One

of its primary contributions is the provision of filters that are rigorously localized. This means that the influence of a filter at a central vertex is limited to a disk of radius K hops, a property that is not inherent in non-parametric spectral filters. In order to accomplish this localization, the filter as shown in Figure 3.3 is parametrized by a polynomial of order K-1 using the Chebyshev expansion, where K denotes the filter's support size.

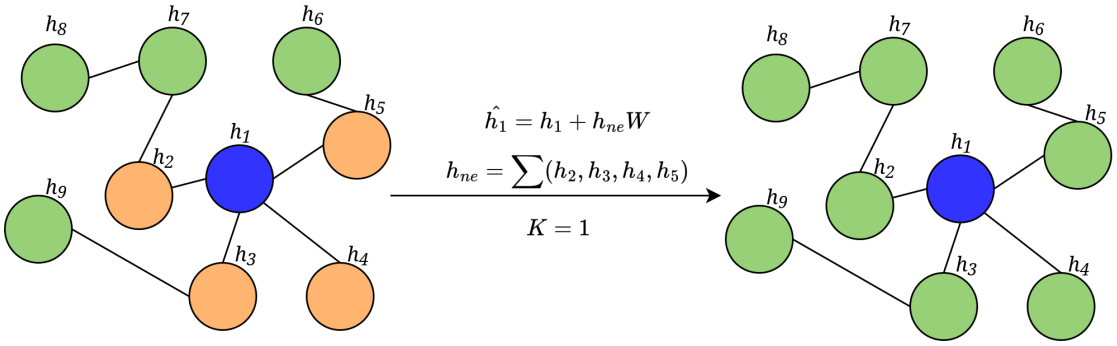

Figure 3.3: Chebyshev Spectral Graph Convolution Network with $K = 1$ configuration

This polynomial parametrization also resolves critical limitations of non-parametric filters, which are not localized and have a learning complexity of $O(n)$, where n is the data dimensionality. In contrast, the Chebyshev-based filter obtains a learning complexity of O(K), akin to classical CNNs. Furthermore, the Chebyshev expansion enables a recursive formulation for rapid filtering, transforming the filtering operation from a costly $O(n^2)$ process (due to multiplication with the graph Fourier basis) to an efficient $O(K|E|)$ operation, where $|E|$ is the number of edges. This method also avoids the computationally costly eigenvalue decomposition (EVD) and the need to store the Fourier basis, which is memory-intensive, particularly for GPUs.

The feature is computed using:

$$\mathbf{X}' = \sum_{k=1}^{K} \mathbf{Z}^{(k)} \cdot \mathbf{\Theta}^{(k)} \tag{3.1}$$

where $\mathbf{Z}^{(k)}$ is computed recursively by:

$$\begin{aligned} \mathbf{Z}^{(1)} &= \mathbf{X} \\ \mathbf{Z}^{(2)} &= \hat{\mathbf{L}} \cdot \mathbf{X} \\ \mathbf{Z}^{(k)} &= 2 \cdot \hat{\mathbf{L}} \cdot \mathbf{Z}^{(k-1)} - \mathbf{Z}^{(k-2)} \end{aligned} \tag{3.2}$$

and $\hat{\mathbf{L}}$ denotes the scaled and normalized Laplacian $\frac{2\mathbf{L}}{\lambda_{\max}} - \mathbf{I}$

3.5 Graph Attention Networks

The Graph Attention Network [68] offers a novel neural network architecture for graph-structured data by employing masked self-attentional layers, directly addressing the drawbacks of earlier methods that depended on graph convolutions or their approximations. As illustrated in Figure 3.4, one of its main characteristics is that it enables nodes to implicitly assign different weights to nodes in their neighborhood without the need for costly matrix operations like inversion or previous knowledge of the network topology. This is achieved by the employment of a graph attentional layer, where each node i and its neighbors $j \in N_i$ undergo a common linear modification (parameterized by weight matrix W) before their characteristics are examined. Attention coefficients e_{ij}, which are determined using a shared attentional process a, then show how important node j's attributes are to node i. By normalizing these coefficients using a softmax function over the neighborhood of node i, α_{ij} is obtained, which is the new feature representation for node i. The transformed neighbor characteristics are then linearly combined using these coefficients as weights. To increase stability and expressive ability, GATs employ multi-head attention, in which numerous distinct attention processes compute characteristics that are then averaged or concatenated.

It is computed as

$$\mathbf{x}_i' = \sum_{j \in \mathcal{N}(i) \cup \{i\}} \alpha_{i,j} \mathbf{\Theta}_t \mathbf{x}_j, \tag{3.3}$$

where the attention coefficients $\alpha_{i,j}$ are computed as

$$\alpha_{i,j} = \frac{\exp\left(\text{LeakyReLU}\left(\mathbf{a}_s^\top \mathbf{\Theta}_s \mathbf{x}_i + \mathbf{a}_t^\top \mathbf{\Theta}_t \mathbf{x}_j\right)\right)}{\sum_{k \in \mathcal{N}(i) \cup \{i\}} \exp\left(\text{LeakyReLU}\left(\mathbf{a}_s^\top \mathbf{\Theta}_s \mathbf{x}_i + \mathbf{a}_t^\top \mathbf{\Theta}_t \mathbf{x}_k\right)\right)} \tag{3.4}$$

3.6 Transfer Learning

A transfer learning based approach uses a model created for one task as the starting point for a model on another related task, the target task [71]. Transfer learning enables the knowledge stored in a pre-trained model to be utilized and optimized for the target domain, as opposed to training a model from scratch, which often requires substantial volumes of labeled data and computational resources. Formally, transfer learning seeks to enhance the learning of the target predictive function $f_T(\cdot)$ in $\mathcal{D}_T$

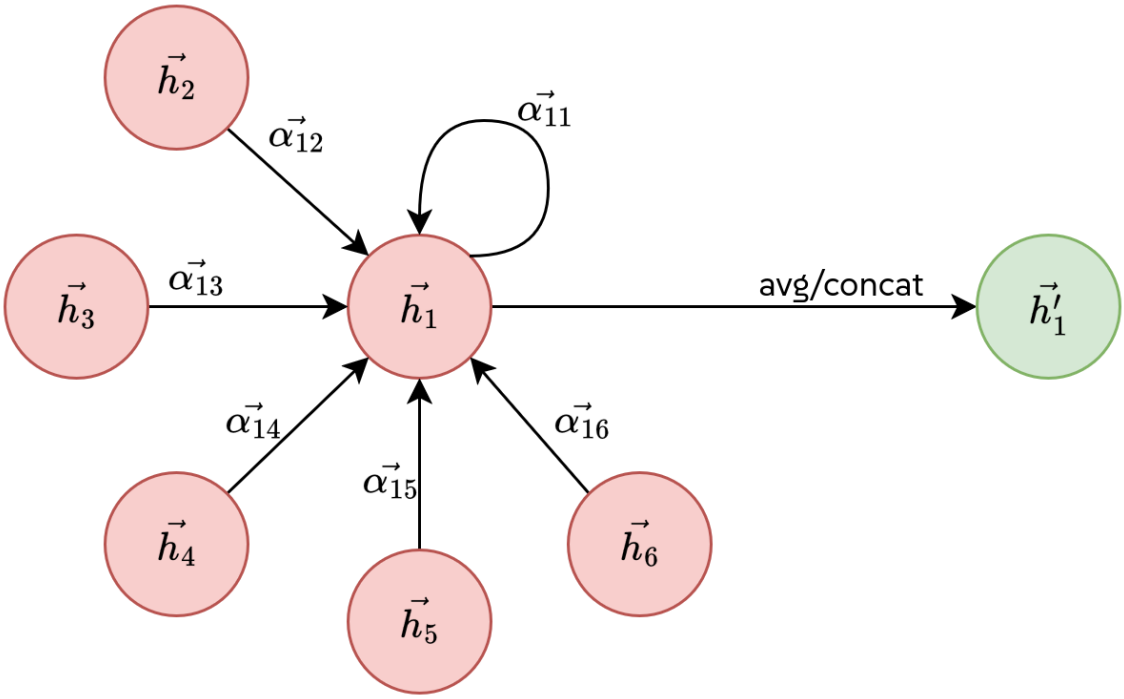

Figure 3.4: An illustration of multi-head attention (with $K = 3$ heads) by node 1 on its neighborhood

using the knowledge from $\mathcal{D}_S$ and $\mathcal{T}_S$, where $\mathcal{D}_S \neq \mathcal{D}_T$ or $\mathcal{T}_S \neq \mathcal{T}_T$ [46]. Reusing the learnt parameters (such as convolutional filters or feature extractors) from the source model and modifying them for the new task by freezing, partially freezing, or fine-tuning the layers is the most popular method. This procedure is particularly helpful in fields with a lack of labeled data [64]. Figure 3.5 illustrates the complete procedure used in this operation.

3.7 Enhanced GCN Model Architecture

The illustrated model architecture represents a multi-branch Graph Convolutional Network specifically designed for the binary classification of Autism Spectrum Disorder and Typically Developing individuals. The model is built upon a graph-based learning paradigm, integrating multimodal brain imaging and phenotypic data, and employs both spectral graph convolution operations and graph attention mechanisms to effectively learn from relational and feature-specific representations.

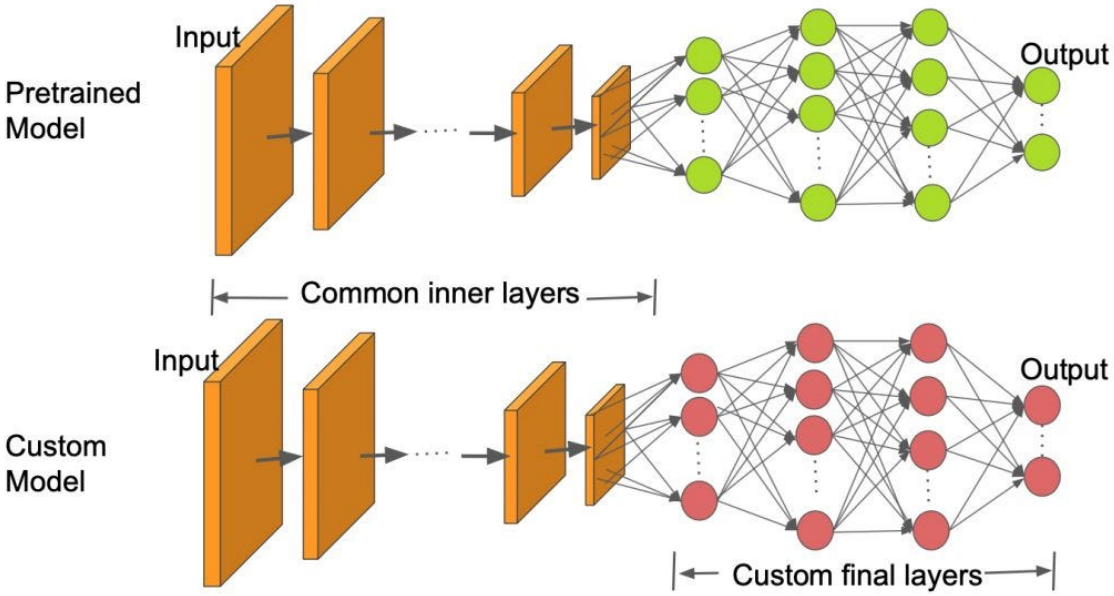

Figure 3.5: Demonstration of transfer learning where the pre-trained model acts as the basis of knowledge transfer for the custom model

3.7.1 Input Modality

At the input stage, the architecture accepts three distinct data modalities collected from a cohort of 870 subjects. These include functional MRI (fMRI) data with a dimensionality of 870×4000, structural MRI features with dimensions of 870×1200, and phenotypic data consisting of six features (age, gender, FIQ, NUM, PEC, and RAT) for each subject, yielding a total of 870×6. Each modality is processed independently through its respective branch, reflecting the modular and scalable design of the network that allows each type of data to undergo specialized

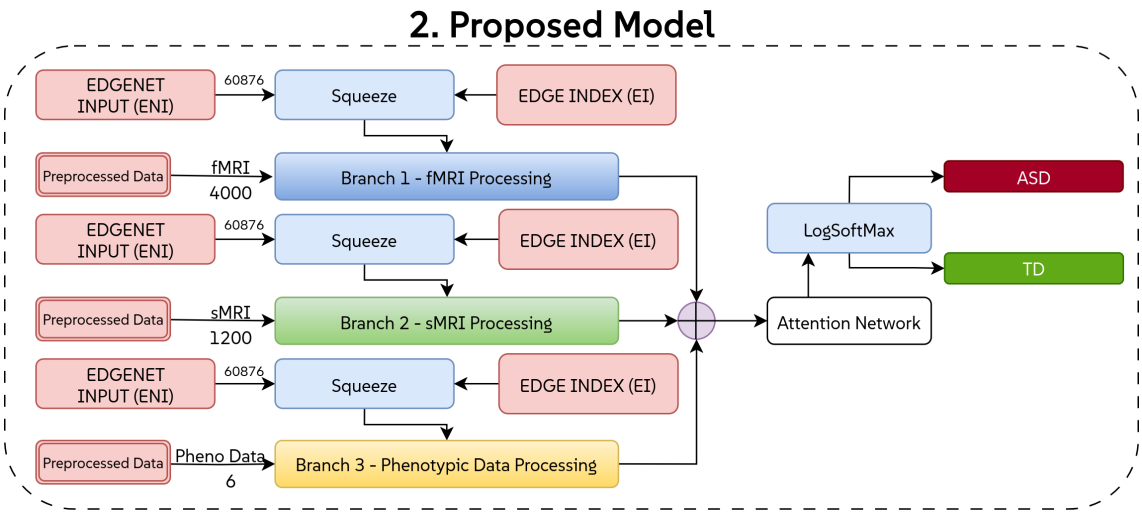

Figure 3.6: Proposed model for the ASD classification task

graph convolutional transformations.

3.7.2 Branched Graph Convolution

Within each branch, the architecture utilizes graph connectivity information encoded via an EDGE INDEX and EDGENET INPUT, the latter consisting of $60,876$ pairwise connections between subjects. Prior to feature processing, the EDGENET INPUT is dimensionally aligned using a Squeeze operation. Subsequently, each modality-specific branch employs two successive Chebyshev Graph Convolutional layers (ChebConv), which are spectral convolution operations that leverage Chebyshev polynomials to approximate graph Fourier filters. The first ChebConv layer transforms the input into a 32-dimensional feature space for each subject (i.e., 870×32), followed by a ReLU non-linearity. A second ChebConv layer further processes the output, again followed by ReLU activation. Notably, residual connections are integrated by summing the outputs of the two convolutional stages, which facilitates gradient flow and stabilizes training, particularly in deeper architectures.

3.7.3 Branch Concatenation

Upon completion of individual processing in each branch, the resulting feature representations (each of dimension 870×32) are concatenated along the feature dimension to yield a unified embedding of size 870×96. This concatenated multi-modal representation is subsequently normalized using Batch Normalization (BatchNorm), a standard practice to accelerate convergence and maintain stable distributions of activations. A Dropout layer follows, which serves as a regularization mechanism by randomly zeroing a fraction of the feature activations during training, thereby reducing the risk of overfitting.

3.7.4 Graph Attention

The architecture then applies a Graph Attention Convolution (GATConv) layer to the fused representation. GATConv introduces an attention mechanism that enables the model to assign varying degrees of importance to neighboring nodes in the graph, thereby selectively aggregating the most informative features from connected subjects. The output of the attention layer retains the dimensionality of 870×96 and is combined with its input through a residual connection, further enhancing model robustness and expressiveness.

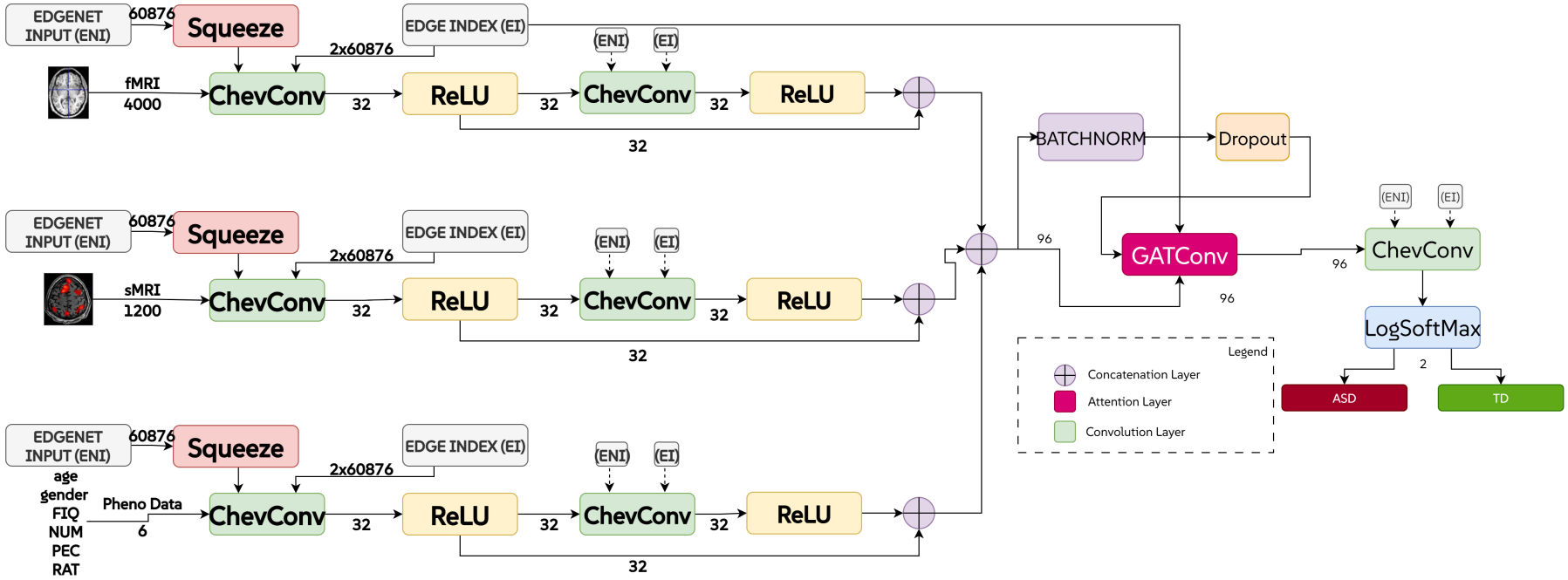

Figure 3.7: Composition of proposed enhanced GCN architecture

In the final stage of the network, the attention-refined features are passed through an additional ChebConv layer that reduces the dimensionality from 96 to 2, aligning with the binary nature of the classification task. The network then applies a LogSoftmax activation function, converting the final feature representation into log-probabilities corresponding to the two output classes: ASD and TD.

3.7.5 Final Output

The final output of the model is a matrix of shape 870×2, where each row corresponds to a subject and contains the log-probabilities of that subject being classified as either ASD or TD. This architecture effectively combines modality-specific graph convolutional learning with attention-based feature refinement, allowing it to capture complex interactions across heterogeneous neuroimaging and demographic data. Its design underscores the strengths of graph-based deep learning in modeling relational data structures inherent in population-based neurological studies.

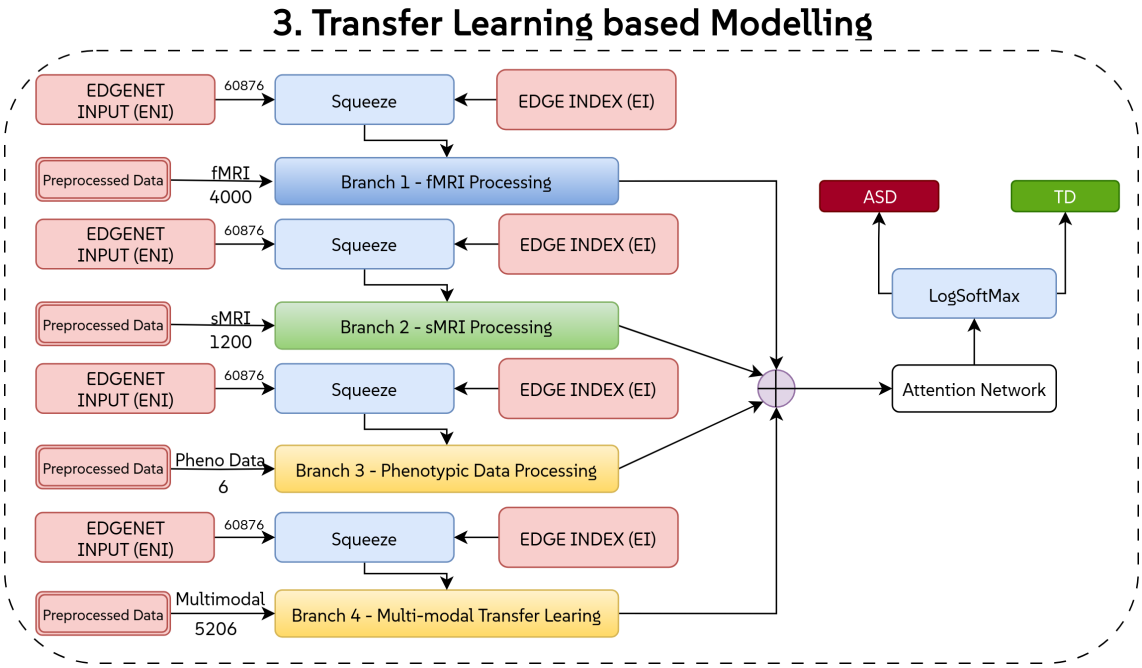

Figure 3.8: Transfer learning based approach for the proposed methodology

3.7.6 Transfer Learning based GCN architecture

To enable transfer learning on the existing multi-branched GCN, a transfer learning approach was undertaken by appending a separate branch to the main proposed architecture. The architecture illustrated in Figure 3.9 embodies a transfer learning framework that integrates multimodal neuroimaging and phenotypic data through

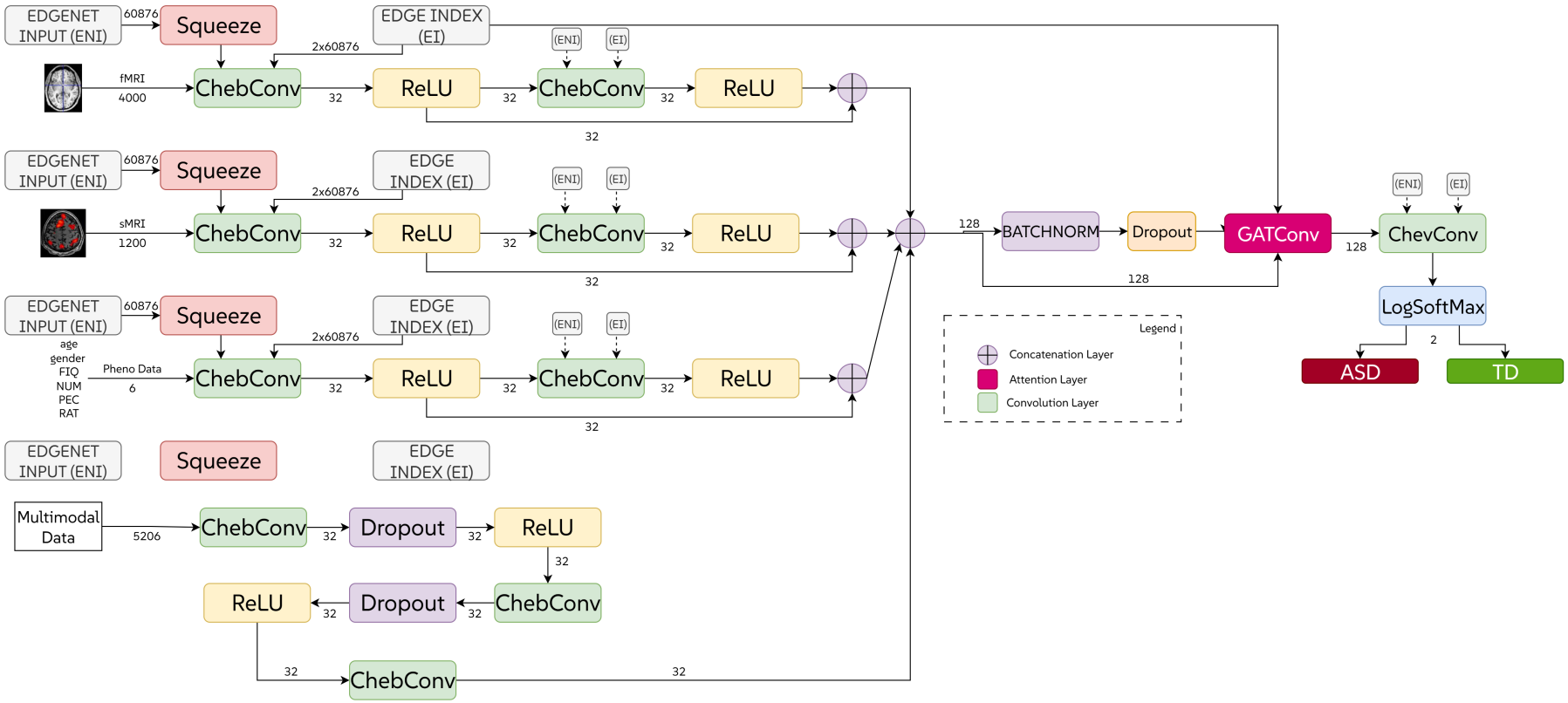

Figure 3.9: Transfer learning-based multimodal GCN architecture

graph-based convolutional processing. This model utilizes a combination of feature extractors, specifically Chebyshev convolutional layers (ChevConv), to process functional MRI (fMRI), structural MRI (sMRI), and phenotypic data streams. Each modality is independently subjected to a graph representation defined by a shared edge index input, denoted as ENI and EI, followed by sequential convolution and non-linear activation layers. After two stages of graph convolutional transformation with ReLU activations, the resulting features from each stream are concatenated and passed through a shared normalization and regularization pathway involving Batch Normalization and Dropout layers. A Graph Attention Convolutional Layer (GATConv) is then employed to enhance discriminative representation by adaptively weighting the contributions of neighboring nodes. The final layer of the network is a task-specific ChevConv block, followed by a LogSoftMax activation to produce class probabilities for the target classification task (Autism Spectrum Disorder vs. Typically Developing. The lower pathway in the model represents a transfer learning stream that accepts pre-processed multimodal features, which are passed through a shallow ChevConv stack and subsequently merged with the main architecture. The complete parameter list is available in Table 3.2. This design enables the reuse of knowledge from previously trained modalities or tasks, effectively enhancing generalization and robustness in low-data regimes typical in neuroimaging-based clinical classification.

Table 3.2: Architecture and parameter breakdown of the Enhanced GCN with Transfer-learning based approach model.

Layer	Input Shape	Output Shape	#Param
EnhancedGCN	[870, 5206], [2, 60876], [60876], [870, 5206]	[870, 2]	1,388,194
(branch1_conv1)ChebConv	[870, 5000], [2, 60876], [60876]	[870, 32]	320,032
(branch1_conv2)ChebConv	[870, 32], [2, 60876], [60876]	[870, 32]	5,152
(branch2_conv1)ChebConv	[870, 994], [2, 60876], [60876]	[870, 32]	63,648
(branch2_conv2)ChebConv	[870, 32], [2, 60876], [60876]	[870, 32]	5,152
(branch3_conv1)ChebConv	[870, 6], [2, 60876], [60876]	[870, 32]	416
(branch3_conv2)ChebConv	[870, 32], [2, 60876], [60876]	[870, 32]	5,152
(gcn_branch)GCNBranch	[870, 5206], [2, 60876], [60876]	[870, 32]	970,336
(conv1)ChebConv	[870, 5206], [2, 60876], [60876]	[870, 32]	960,032
(conv2)ChebConv	[870, 32], [2, 60876], [60876]	[870, 32]	5,152
(conv3)ChebConv	[870, 32], [2, 60876], [60876]	[870, 32]	5,152
(relu)ReLU	[870, 32]	[870, 32]	–
(dropout)Dropout	[870, 32]	[870, 32]	–
(att)GATConv	[870, 128], [2, 60876]	[870, 128]	16,768
(conv_final)ChebConv	[870, 128], [2, 60876], [60876]	[870, 2]	1,282
(relu)ReLU	[870, 32]	[870, 32]	–
(dropout)Dropout	[870, 128]	[870, 128]	–
(batch_norm)BatchNorm1d	[870, 128]	[870, 128]	256
(softmax)LogSoftmax	[870, 2]	[870, 2]	–

3.8 Training, Testing, and Validation

To achieve a reliable and unbiased estimation of the models predictive performance, a stratified 5-fold cross-validation procedure was implemented. In this approach, the dataset was partitioned into five mutually exclusive and approximately equal-sized subsets, ensuring that the class distribution within each subset was consistent with the overall dataset distribution.

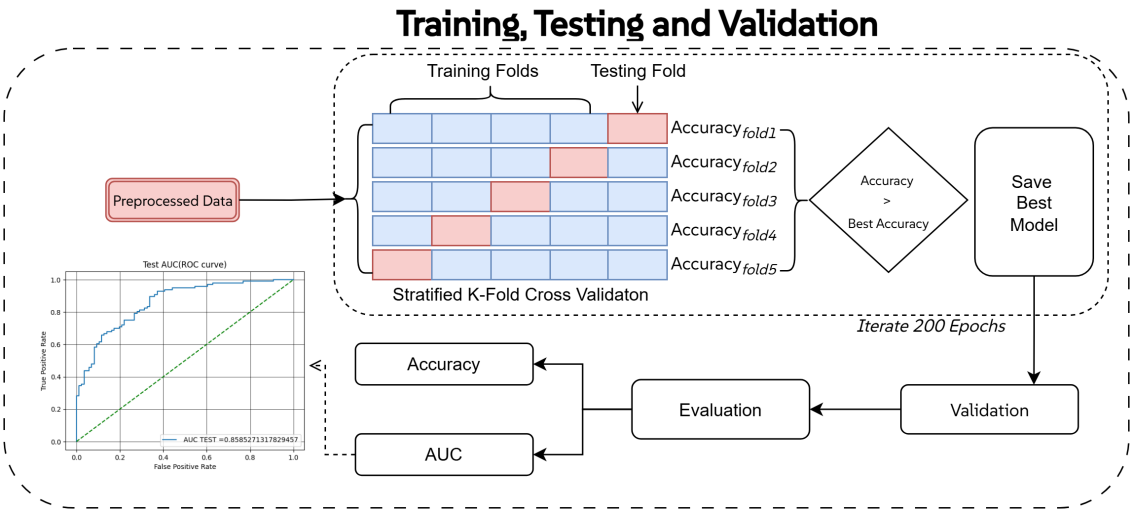

Figure 3.10: Training, testing and validation phase of the proposed enhanced GCN pipeline

For each fold, the subset was designated as the validation set, while the remaining four subsets were combined to form the training set. The model was trained on and subsequently evaluated on. This process was repeated iteratively such that each subset served as the validation set exactly once.

This averaging process mitigates the impact of variance introduced by any particular train-validation split and provides a more stable and generalizable performance estimate. By employing stratification, the method also ensured that class imbalance did not introduce bias into the validation process, thereby maintaining the integrity of the model evaluation.

Following the footsteps of previous influential works in the domain, there was no separate testing set designated for the experimentation. Rather, the training phase was incorporated such that, for each fold of the cross-validation step, one fold was kept as the testing fold, and the rest four were used as the training folds. In order to keep the samples distributed, a stratified cross-validation was employed.

Chapter 4

Experimental Design

The experimental framework is designed to evaluate the proposed enhanced GCN architecture for classifying Autism Spectrum Disorder using neuroimaging and phenotypic data. The study is conducted using data from the ABIDE I dataset, which includes resting-state functional MRI (fMRI), structural MRI (sMRI), and six types of phenotypic information. The pipeline comprises several interconnected stages including data preprocessing, feature extraction, population graph construction, model training with cross-validation, and ensemble learning via max voting.

4.1 Feature Extraction

The fMRI features are extracted from subject-specific connectivity matrices derived from the CC200 atlas. For each subject, the upper triangular portion of the connectivity matrix (excluding the diagonal) is flattened into a one-dimensional vector, resulting in 19,900 features when using the CC200 atlas. These features are scaled using the RobustScaler to mitigate the effects of outliers. The sMRI features are generated using FreeSurfer-derived statistical outputs across three categories: cortical thickness from the Desikan-Killiany atlas, volumetric information from the ASeg atlas, and white matter parcellations from the WMPARC atlas. Each of these sources provides hundreds of features-612 from Desikan-Killiany, 315 from aseg, and 490 from wmparc-yielding a combined sMRI feature dimension of 1,417. These features are normalized using the StandardScaler to ensure zero-mean, unit-variance scaling across features.

Phenotypic data consist of six variables: age, gender, full-scale IQ (FIQ), numerical reasoning (NUM), perceptual reasoning (PEC), and reaction time (RAT). Missing

values for FIQ are replaced with a default of 108, and all features except gender and RAT are standardized.

4.2 Graph Building

Graph-based learning is facilitated by constructing a population graph, where nodes represent subjects and edges indicate similarity based on site membership. The graph is encoded as an adjacency matrix, which is further transformed into ‘edge_index‘ and ‘edgenet_input‘ tensors for use within the PyTorch Geometric framework. Only edges with a similarity score exceeding a threshold of 0.99 are retained to ensure strong relational ties.

4.3 Feature Selection

Feature selection is conducted independently for fMRI and sMRI data using the ‘SelectKBest‘ method based on the ANOVA F-statistic. This process is performed separately for each fold in the cross-validation scheme to prevent data leakage. A five-fold stratified cross-validation is employed, with stratification based on both diagnosis and acquisition site to ensure balanced data splits across folds. For each fold, training, validation, and test indices are maintained separately, and the test sets are non-overlapping with training sets from other folds. The final input vector per subject includes 4,000 selected fMRI features, 1,200 selected sMRI features, and 6 phenotypic features, amounting to a total of 5,206 dimensions.

The GCN model architecture includes three modality-specific branches with Chebyshev Spectral Convolutional layers (ChebConv) for each input type: fMRI (870×4000), sMRI (870×1200), and phenotypic (870×6). Each branch uses two ChebConv layers with residual connections. The outputs are concatenated and passed through batch normalization and dropout layers before being processed by a Graph Attention Network layer. A final ChebConv layer maps the 96-dimensional combined feature space to a 2-dimensional output, followed by a LogSoftmax activation to produce log-probabilities.

4.4 Chebyshev Convolution Order Configuration

In the proposed GCN architecture, the choice of polynomial orders $K_1 = 2$ and $K_2 = 5$ is motivated by the need to balance local feature extraction with broader

structural awareness of the graph. Within Chebyshev spectral convolution, the parameter K determines the size of the receptive field, thereby controlling the extent to which node representations are influenced by their neighbors. A smaller order, as employed in the first convolutional layer with $K_1 = 2$, restricts the operation to two-hop neighborhoods. This design encourages the preservation of local structural patterns and reduces the risk of oversmoothing in the initial stages of feature transformation. In contrast, the second convolutional layer is configured with a larger order, $K_2 = 5$, enabling the model to integrate information from up to five-hop neighborhoods. This broader receptive field facilitates the capture of higher-order dependencies and more global contextual information across the graph. By combining these two configurations, the model benefits from a multi-scale representation, in which local details are preserved while complementary global features are progressively incorporated. Such a branched design enhances the expressive power of the network and contributes to more robust representation learning.

4.5 Graph Attention Layer

In the multi-branch graph convolutional network, a GATConv layer with three attention heads was employed to adaptively weight neighborhood contributions, allowing the model to emphasize informative connections while suppressing noise. The use of multiple heads enables the network to capture diverse relational patterns, stabilizes learning, and enhances generalization. This design ensures more robust and discriminative feature extraction across branches, which is particularly valuable for complex tasks.

4.6 Experimental Design

To comprehensively evaluate the proposed framework for Autism Spectrum Disorder classification using the ABIDE I dataset, two primary experimental strategies were adopted.

4.6.1 Modality-Specific Experiment

This set of experiments aimed to assess the contribution of individual modality combinations to the overall classification performance. Specifically, pairwise combinations of the available modalitiesresting-state functional MRI (fMRI),

structural MRI (sMRI), and phenotypic (Phe) datawere evaluated. The rationale for this approach was to determine whether the integration of all modalities provides a significant advantage over using only subsets of the data. By comparing the classification results across different pairwise configurations, the necessity and effectiveness of incorporating all available modalities were quantitatively justified.

4.6.2 Architecture-Specific Experiment

To investigate the influence of architectural choices on model performance, experiments were conducted using the proposed Enhanced Graph Convolutional Network under different configurations. First, the baseline Enhanced GCN was evaluated without the incorporation of Graph Attention Networks. Subsequently, the Enhanced GCN was augmented with GAT layers to exploit node-level attention mechanisms for improved feature aggregation. Additionally, hyperparameter tuning was performed to optimize learning rates, weight decay, dropout rates, and hidden layer dimensions. This design allowed for a systematic comparison of architectural variants and parameter settings, ensuring that performance improvements could be attributed to the architectural enhancements rather than incidental factors.

4.7 Hardware and Software requirements

The experiment was conducted using Google Colaboratory. A tesla T4 GPU was employed to carry out computations in the GPU of the virtual machine. The experiment required $\approx$ 4 GB of RAM and $\approx$ 8 GB of GPU to execute the tasks. The total runtime for each fold of the training phase was around 10 minutes, making the whole 5-fold cross-validation training phase run within an hour.

4.8 Model Training

Model training employs the Stochastic Gradient Descent (SGD) optimizer with momentum and Nesterov acceleration. The learning rate is regulated using a Cyclic Learning Rate scheduler with triangular mode. The training loop is executed for 200 epochs per fold, with evaluation at each epoch based on training, validation, and test accuracy and loss. The model epoch yielding the best validation accuracy is saved, and its performance on the test set is logged.

This comprehensive experimental setup ensures rigorous validation of the proposed model, leveraging the strengths of graph-based representation learning and

multi-modal feature integration to advance the classification of ASD from neuroimaging and behavioral data.

4.9 Loss Function

The Negative Log-Likelihood (NLL) loss function is utilized in this model owing to its compatibility with the 'LogSoftmax' output layer, which yields log-probabilities for binary classification. NLL loss effectively evaluates the disparity between the predicted log-probabilities and the real class labels, consistent with the principles of maximum likelihood estimation. This decision offers a probabilistically grounded learning objective, while also delivering numerical stability and computing efficiency, particularly when dealing with tiny probability values. Furthermore, NLL permits quick gradient calculation and is well-suited for classification problems involving categorical targets, making it an acceptable and theoretically sound loss function for the ASD classification framework. NLL is given by:

$$\text{NLL Loss} = -\sum_{i=1}^{N} \log p(y_i \mid x_i) \tag{4.1}$$

where $p(y_i \mid x_i)$ represents the predicted probability for the true label y_i of instance x_i, and N is the total number of samples.

4.10 Cross-validation testing

For model training in the ASD detection task, a five-fold stratified cross-validation framework was employed to maximize data utilization and ensure robust generalization. The entire dataset was partitioned into five mutually exclusive subsets of approximately equal size. Stratification was applied to preserve the overall proportion of ASD and control subjects within each subset, thereby maintaining class balance across all folds.

During each cross-validation iteration, four subsets were aggregated to form the training set, while the remaining subset was withheld for evaluation. The model was trained exclusively on the training set in that iteration, with parameters reinitialized before each fold to avoid carryover effects. This process was repeated five times, allowing the model to be trained and validated on distinct, non-overlapping data splits.

The stratified cross-validation training process ensures that every subject in the dataset contributes to both model learning and validation while mitigating the risk of biased performance estimates due to imbalanced class distributions. Final performance metrics were obtained by aggregating the evaluation results across all folds, providing a statistically reliable assessment of the models classification capability.

4.11 Evaluation Metrics

Accuracy and the Area Under the Receiver Operating Characteristic Curve (AUC-ROC), two metrics that offer complementary insights into categorization quality, are used to assess the model's performance. According to (4.2), accuracy is the ratio of successfully predicted labels to all predictions, which can be computed as follows:

$$\text{Accuracy} = \frac{TP + TN}{TP + TN + FP + FN} \tag{4.2}$$

where true positives, true negatives, false positives, and false negatives are indicated by the symbols TP, TN, FP, and FN, respectively. Although accuracy provides a clear indicator of general correctness, unbalanced datasets may cause bias. The model additionally assesses the Negative Log-Likelihood (NLL) Loss, as shown in (4.1), which measures the discrepancy between the actual class labels and the predicted log-probabilities in order to account for probabilistic performance. Last but not least, the AUC-ROC metric, which is developed in (4.3), plots the True Positive Rate (TPR) against the False Positive Rate (FPR) across a range of threshold values to capture the model's capacity for class discrimination. Formally, the AUC is stated as:

$$\text{AUC} = \int_0^1 \text{TPR}(FPR^{-1}(x))\, dx \tag{4.3}$$

where $\text{TPR} = \frac{TP}{TP+FN}$ and $\text{FPR} = \frac{FP}{FP+TN}$ are the definitions of TPR and FPR, respectively. AUC offers a threshold-independent evaluation of classifier performance; higher discriminative capability is shown by values nearer 1. When combined, these measures provide a thorough assessment of the model's classification accuracy, probabilistic confidence, and capacity to differentiate between those with ASD and those who are typically developing.

4.12 Hyper-parameter Settings

The model training method involves careful specification and, in certain instances, adjustment of multiple important hyperparameters to enhance performance. The summary of the chosen hyperparameters is available in Table 4.1. The Graph Convolutional Network architecture was set with an input dimension of 5206, a hidden dimension of 32, and an output dimension of 2. For its Chebyshev convolutional layers, the orders K_1 and K_2 were set to 2 and 5, respectively. An initial dropout rate of 0.5 was adopted during single-fold training.

Table 4.1: Summary of hyperparameters used in model training

Parameter	**Value**
Input dimension	5206
Hidden dimension	32
Output dimension	2
Chebyshev order K_1	2
Chebyshev order K_2	5
Dropout rate (initial)	0.5
Optimization	
Optimizer	Stochastic Gradient Descent (SGD)
Learning rate	1×10^{-3}
Momentum	0.8
Nesterov acceleration	Enabled
Weight decay	1.0
Learning Rate Scheduler	
Scheduler type	Cyclic learning rate
Base learning rate	1×10^{-3}
Maximum learning rate	1×10^{-7}
Mode	Triangular
Step size (up-cycle)	500
Step size (down-cycle)	300
Regularization and Stability	
Gradient clipping max norm	2.0

For the optimization method, the training phase consistently applied the Stochastic Gradient Descent (SGD) optimizer. This SGD optimizer was configured with a learning rate of $1e^{-3}$, a momentum of 0.8, Nesterov acceleration, and a weight decay of 1.0. Learning rate changes were controlled by a cyclic learning rate scheduler, which had a base learning rate of $1e^{-3}$, a maximum learning rate of $1e^{-7}$, a triangular mode, and step sizes of 500 for up-cycle and 300 for down-cycle phases. Additionally, gradient clipping with a maximum norm of 2.0 was applied to stabilize training.

Chapter 5

Results and Discussion

Here, we report the results obtained from extensive experimentation on the ABIDE I dataset. Along with the quantitative results, a comprehensive comparison with the state-of-the-art research on the specific problem domain is also available in Table 5.3. The state-of-the-art performance quantities are reported as found in their original manuscripts.

5.1 Ablation Study

Along with a comparison among the state-of-the-art works, we also validated the enhanced GCN architecture using a varied ablation study. Here in Table 5.1, a quantitative analysis of different configurations of the model architecture is available. As evident from the results, the necessity to add each component of the architecture is feasible and proves to be a crucial part in the overall result composition.

The ablation study presented in Table 5.1 systematically evaluates the contributions of individual enhancements to the proposed Enhanced Graph Convolutional Network (EGCN) architecture by examining four model variants across test accuracy (ACC) and Area Under the ROC Curve (AUC). The baseline EGCN incorporating the Graph Attention Network layer achieves a test accuracy of 70.14% and an AUC of 0.78, reflecting marginal improvements of 1.54% in ACC and 3.79% in AUC over the standard GCN. Notably, removing the GAT module (EGCN w/o GAT) yields a slight performance gain, with test accuracy rising to 71.24% and AUC to 0.80, suggesting that attention mechanisms alone may not consistently improve model generalization. However, the integration of GAT without hyperparameter tuning

Table 5.1: Ablation study of different enhanced GCN modifications along with baseline comparison

Model	Val ACC	Val AUC	Val ACC Inc.(%)		Val AUC Inc. (%)	
			GCN[15]	Ensemble GCN[15]	GCN[15]	Ensemble GCN[15]
EGCN w GAT	70.14%	0.78	1.54%	-1.16%	3.79%	-0.01%
EGCN w/o GAT	71.24%	0.80	2.64%	-0.06%	5.45%	1.65%
EGCN w GAT w/o HPT	72.43%	0.81	3.83%	1.13%	6.33%	2.53%
EGCN w GAT w HPT	**74.82%**	**0.82**	6.21%	3.51%	7.33%	3.53%
EGCN w GAT w HPT w TL	**72.89%**	**0.79**	4.29%	1.59%	5.00%	1.00%

(HPT) further elevates performance to 72.43% test accuracy and 0.81 AUC, indicating that architectural complexity contributes positively even without optimized parameters. The full model, EGCN with both GAT and hyperparameter tuning (EGCN w GAT w HPT), achieves the highest performance, with a test accuracy of 74.82% and AUC of 0.82. This corresponds to a substantial improvement of 6.21% and 7.33% in ACC and AUC, respectively, over the baseline GCN, and 3.51% and 3.53% over the Ensemble GCN. Also, the transfer learning based approach achieved an accuracy of 72.89% and an AUC of 0.79. Compared to the only available literature on transfer learning in GCN-based models, the performance of the proposed model is quite substantial, with a increment of 14.59% increment in ACC and a 21% increment in AUC. These findings underscore the compounded benefits of both architectural enhancements and rigorous hyperparameter optimization in achieving superior classification performance in ASD prediction.

Another ablation study was performed to systematically evaluate the contribution of different modality combinations in the ABIDE I dataset to the classification performance of the proposed model. The investigated modalities included resting-state functional MRI (fMRI), structural MRI (sMRI), and phenotypic (Phe) data, tested in various pairwise and multi-modal configurations and is reported in Table 5.2. The results demonstrate that integrating all three modalities (fMRI, sMRI, and Phe) yields the highest performance, achieving an accuracy of 74.82% and an AUC of 0.82, indicating a substantial improvement over any two-modality combination. Specifically, fMRI combined with sMRI achieved an accuracy of 65.23% and an AUC of 0.71, closely followed by the fMRI + Phe pairing with 65.04% accuracy and the same AUC. The sMRI + Phe combination yielded the lowest performance, with 61.89% accuracy and an AUC of 0.67. These findings highlight the complementary nature of the three modalities and emphasize the advantage of multi-modal integration for enhanced diagnostic performance in the ABIDE I dataset.

Table 5.2: Ablation study on different modalities of the ABIDE I dataset

Model	**Modality**	**Accuracy**	**AUC**
Proposed Model	fMRI + sMRI	65.23%	0.71
	fMRI + Phe	65.04%	0.71
	sMRI + Phe	61.89%	0.67
	fMRI + sMRI + Phe	**74.82%**	**0.82**

Table 5.3: Performance Comparison with state-of-the-art works on ASD classification

Ref.	Year	Model	Testing Subset	Test ACC	Test AUC
Abbas et. al [2]	2023	Multi-modal CNN	Partial	75.14%	0.77
Wang et. al [69]	2023	Weight Learning DeepGCN	Partial	77.27%	0.82
Zhang et. al. [75]	2024	LGMDA-SACDL	Partial	75.32%	0.75
Saponaro et. al [55]	2024	FR-NN with C-NN	Partial	85.02%	0.78
Ma et. al [41]	2024	Multi-atlas Fusion Template with GCN	Partial	75.70%	0.73
Gupta et. al [24]	2025	TinyViT	Partial	76.62%	-
Dong et. al.[15]	2025	GCN	Complete	68.60%	0.74
Dong et. al.[15]	2025	Ensemble GCN	Complete	71.30%	0.78
Heinsfeld et. al.[29]	2018	Autoencoder based DNN	Complete	65.00%	-
Du et. al. [18]	2022	SVM-RFE	Complete	72.10%	-
Song et. al [59]	2024	MMGCN	Complete	72.37%	0.76
Du et. al [17]	2025	FCN based model	Complete	68.98%	-
Proposed	2025	**Enhanced GCN With GA**	Complete	**74.81%**	**0.82**
Li et al. [35]	2022	Ensemble GCN and TL	Complete	58.30%	0.57
Proposed	2025	**Enhanced GCN With GA and TL**	Complete	**72.89%**	**0.79**

5.2 Comparison with the state-of-the-art methods

Table 5.3 presents a comprehensive comparison of the proposed Enhanced GCN with Graph Attention model against several state-of-the-art GCN-based and deep learning models for ASD classification. The proposed model achieves a test accuracy of 74.81% and an AUC of 0.82 on the complete ABIDE dataset, outperforming several baseline and advanced methods. When compared to Dong et al. [15], whose standard GCN and Ensemble GCN models achieved 68.60% and 71.30% accuracy, respectively, the proposed model exhibits a notable performance gain, particularly in AUC, where it surpasses both baselines by 8 and 4 percentage points, respectively. Additionally, the model outperforms other GCN variants such as MMGCN (72.37% accuracy, 0.76 AUC) proposed by Song et al. [59], and FCN-based architectures like that of Du et al. [17] with 68.98% accuracy. Among multimodal models trained on partial datasets, the proposed method demonstrates comparable or superior performance to architectures such as the Multi-modal CNN (75.14% accuracy, 0.77 AUC) by Abbas et al. [2], and Weight Learning DeepGCN (77.27% accuracy, 0.82 AUC) by Wang et al. [69]. Although the model by Saponaro et al. [55] reports a higher accuracy of 85.02%, it is important to note that it is evaluated on a partial subset, which may limit its generalizability. The proposed model maintains state-of-the-art performance with balanced accuracy and AUC on the complete dataset, affirming the effectiveness of graph attention integration and multi-modal learning in enhancing ASD classification.

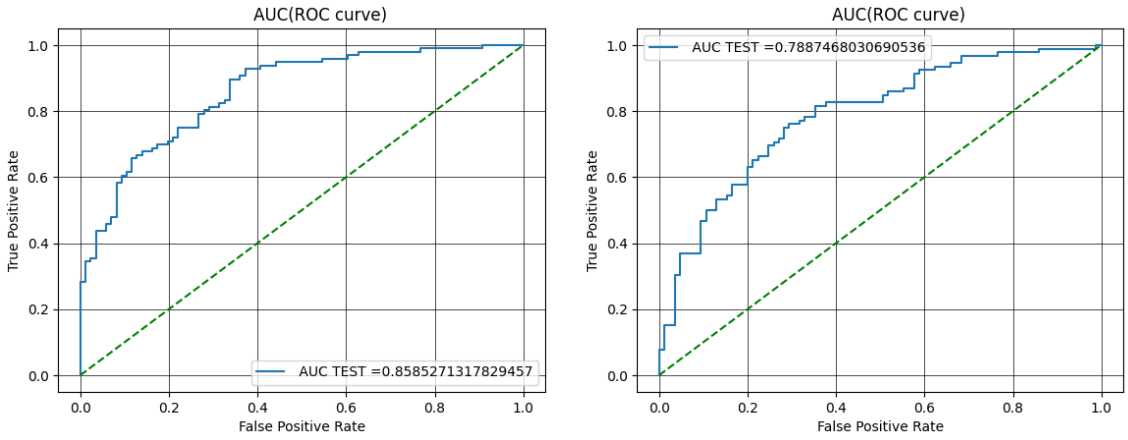

(a) Best AUC using Enhanced GCN with GAT and HPT

(b) Best AUC using Enhanced GCN with GAT and HPT and TL

Figure 5.1: Qualitative results depicted using Best AUC curve obtained during training phase

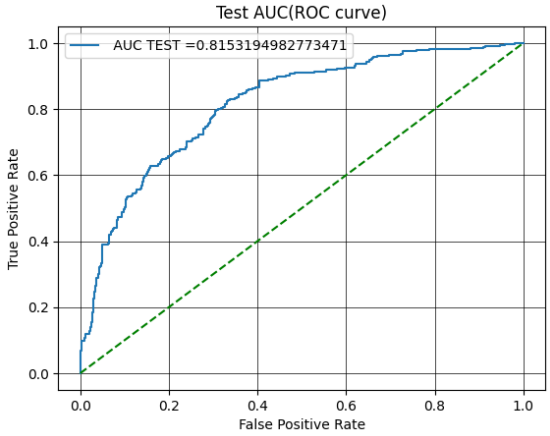

(a) Testing AUC using Enhanced GCN with attention

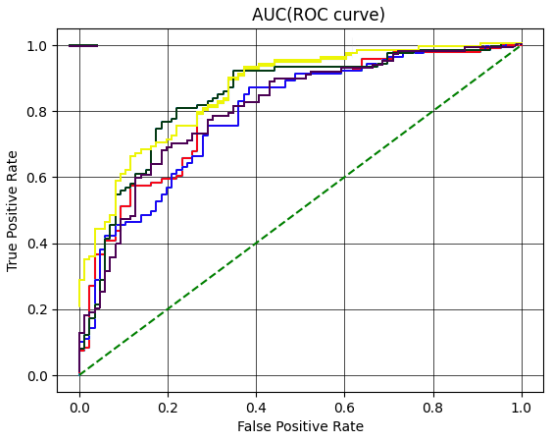

(b) Training AUC using Enhanced GCN with attention

Figure 5.2: Qualitative results depicted using the final testing AUC vs five-fold training AUC curve using the proposed Enhanced GCN with attention and hyperparameter tuning

5.3 Performance Evaluation

The performance of the model and its corresponding result analysis is evident from the ROC curve and the loss curve during the experimentation and is presented in Figures 5.1(a), 5.2(a), and 5.4(a). The curves show there was no evident over-fitting and the model performed in a quite stable manner to classify between ASD and TD subjects.

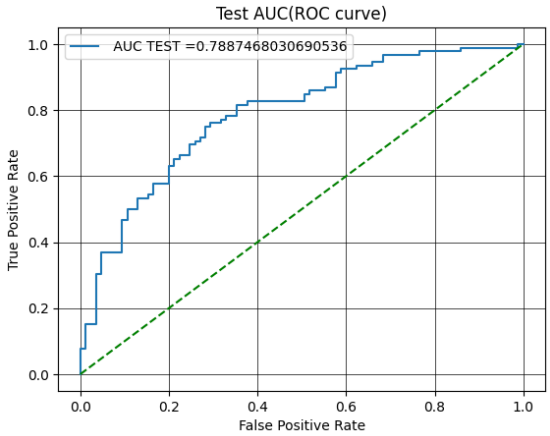

(a) Testing AUC using Enhanced GCN with attention and transfer learning

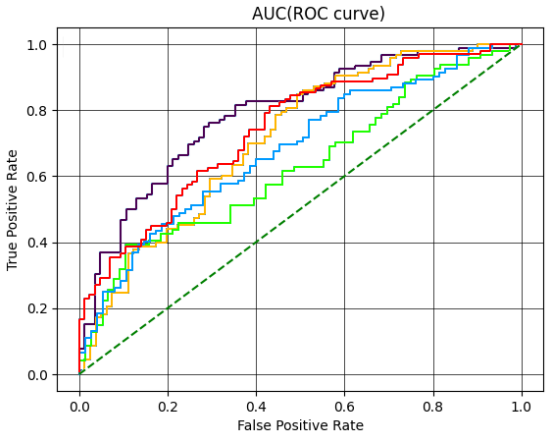

(b) Training AUC using Enhanced GCN with attention and transfer learning

Figure 5.3: Qualitative results depicted using the final testing AUC curve vs five-fold training AUC curve using the proposed Enhanced GCN with graph attention and Transfer Learning

5.4 Loss curve analysis

The overall loss curve of the proposed methodology is shown using Figures 5.4(a) and 5.4(b). As we can observe that both graphs depict similar results in the testing vs the training phase, thus we can conclude that there was no evident overfitting, and the model convergence was good. The experimental results for the ASD classification task demonstrate that the training AUC and the 5-fold cross-validation testing AUC values are closely aligned. This consistency across training and testing phases indicates that the proposed model generalizes effectively, capturing underlying patterns in the multimodal graph data rather than overfitting to the training set. The small gap between the two metrics suggests that the chosen architecture, regularization strategies, and feature representations strike an appropriate balance between model complexity and generalization capability.

Importantly, the similarity in performance as shown in Figure 5.4 also reflects the stability of the feature extraction process and the reliability of the preprocessing pipeline, which preserved discriminative patterns across folds. Given that the observed AUC values are consistently high, the results support the suitability of the enhanced GCN architecture and the transfer learning approach for ASD classification. However, the possibility of data leakage or task-specific biases was carefully mitigated through rigorous cross-validation and dataset partitioning. Overall, these findings confirm that the model exhibits robust and reproducible performance, thereby strengthening its potential for real-world applicability in neuroimaging-based ASD detection.

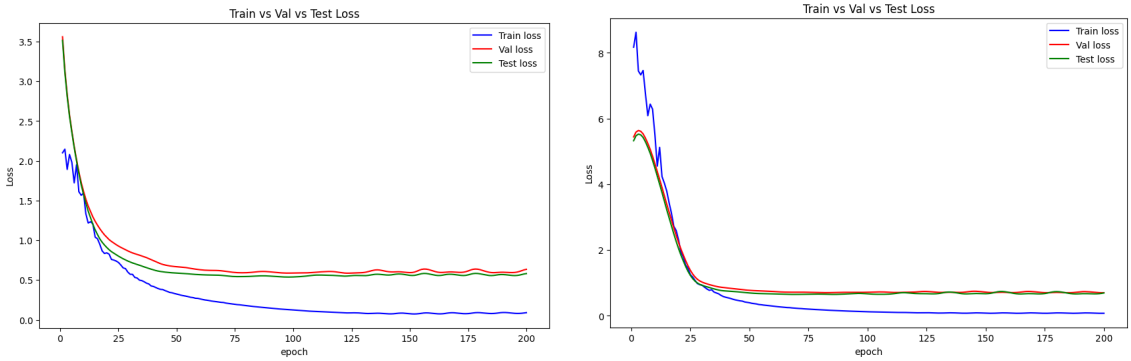

(a) Loss curve using Enhanced GCN with GAT and HPT

(b) Loss curve using Enhanced GCN with GAT and HPT and TL

Figure 5.4: Qualitative results depicted using Train-vs-val-vs-test loss curve during training.

Figure 5.1(a) was obtained in the first fold of cross-validation during the training phase using the proposed enhanced GCN with graph attention and hyper-parameter

tuning. Figure 5.1(b) represents the transfer learning based experimentation qualitative result for the same proposed architecture. Although the final testing AUC, as shown in Figure 5.2(a), is smaller than the one present in Figure 4.3, the close values suggest that the proposed methodology has successfully converged to a solution towards a better result throughout the training epochs. Figure 5.4(a) depicts that the model is devoid of any over-fitting issues and has successfully generalized itself to a state-of-the-art solution for this problem domain.

5.5 Results Discussion

The proposed ASD classification framework excels through a combination of architectural and methodological innovations. Explicit multi-modality handling allows functional MRI, structural MRI, and phenotypic data to be processed through dedicated sub-networks, preserving modality-specific information and reducing cross-modal interference. The integration of Chebyshev Spectral Graph Convolutions with Graph Attention Networks enhances feature learning by combining efficient localized spectral filtering with adaptive neighbor weighting, improving generalization across heterogeneous populations.

High-dimensional neuroimaging and phenotypic data are effectively managed through statistical feature selection (SelectKBest), normalization (StandardScaler, RobustScaler), and architectural regularization via residual connections, mitigating overfitting risks. The graph-based population modeling approach embeds subjects within a relational context, capturing inter-subject dependencies and cohort-level patterns, which improves diagnostic precision.

Performance evaluation confirms that incorporating transfer learning into the enhanced GCN architecture yields notable improvements, achieving 72.89% test accuracy and 0.79 AUC, surpassing multiple state-of-the-art and transfer learning-based baselines. These results validate the effectiveness of combining graph attention mechanisms with transfer learning for robust and generalizable ASD classification.

5.5.1 Performance drop with modality reduction

The results of the ablation study presented in Table 5.2 clearly indicate the substantial influence of multimodal integration on the classification performance. When all three modalitiesfMRI, sMRI, and phenotypic data - were jointly incorporated, the proposed model achieved its highest accuracy of 74.82% and AUC

of 0.82. In contrast, reducing the input to only two modalities resulted in a marked decline in performance, with accuracy dropping to the range of $61.89\% - 65.23\%$ and AUC decreasing to $0.67 - 0.71$. This discrepancy underscores the complementary nature of the different modalities: fMRI provides dynamic functional connectivity patterns, sMRI captures structural variations, and phenotypic data reflects clinical and demographic characteristics. Individually or in pairs, these modalities fail to capture the full spectrum of discriminative information required for robust Autism Spectrum Disorder classification. The drastic change in performance upon modality reduction therefore highlights the necessity of multimodal fusion, as it allows the model to exploit both neuroimaging and non-imaging features, thereby enhancing generalizability and mitigating modality-specific limitations.

5.5.2 Explicit Multi-Modality Handling

The success of the proposed model can be partially attributed to its explicit handling of multiple data modalitiesnamely, functional MRI (fMRI), structural MRI (sMRI), and phenotypic attributesthrough distinct processing branches. By isolating each modality into its dedicated sub-network, the architecture facilitates targeted feature extraction specific to the statistical and spatial properties of that modality. This design not only ensures that the integrity of modality-specific information is preserved but also mitigates cross-modal interference during the learning process. As a result, each data stream contributes uniquely to the final classification task, promoting a more holistic and discriminative representation of Autism Spectrum Disorder-related neuro-biological and behavioral signatures.

5.5.3 Synergy Between Spectral Graph Convolution and Graph Attention

Another key strength of the proposed framework lies in the synergistic integration of Chebyshev Spectral Graph Convolution (ChebConv) layers with Graph Attention Networks. ChebConv enables efficient and localized spectral learning by approximating the graph Fourier basis through Chebyshev polynomials, allowing the model to extract meaningful patterns from graph-structured data with reduced computational overhead. Complementarily, GAT layers incorporate an adaptive attention mechanism that assigns learnable weights to each nodes neighbors, effectively prioritizing more informative connections while down-weighting noisy or weakly correlated relationships. This combination not only enhances the models representational capacity but also enables it to generalize effectively across diverse

and heterogeneous subject populations - a characteristic particularly critical for ASD classification given the disorder's inherent inter-individual variability.

5.5.4 High-Dimensional Feature Handling

Handling the high-dimensional nature of neuroimaging and phenotypic data is a persistent challenge in computational neuroscience. The model addresses this through a multifaceted strategy that includes the use of SelectKBest for statistical feature selection, standardization techniques such as StandardScaler and RobustScaler to normalize feature distributions, and architectural regularization via residual connections. Collectively, these methods allow the network to focus on the most salient and discriminative features, while mitigating risks of over-fitting and variance inflation commonly associated with high-dimensional, low-sample-size datasets. This capability significantly contributes to the robustness and stability of the learning process.

5.5.5 Performance Evaluation of Transfer Learning-based Method

As shown in Table 5.3, the incorporation of transfer learning (TL) into the graph convolutional network framework demonstrates a tangible improvement in model performance. The proposed model variant, *Enhanced GCN with graph attention and transfer learning based approach*, achieves a test accuracy of 72.89% and an AUC of 0.79, indicating a balanced enhancement in both classification precision and discriminatory capability. Notably, this performance surpasses several state-of-the-art models, including the Autoencoder-based DNN (65.00%) [29], SVM-RFE (72.10%) [18], and MMGCN (72.37%) [59]. It significantly outperforms other TL-related models such as the ensemble GCN with TL proposed by Li et al. [35], which yielded only 58.30% accuracy and a notably low AUC of 0.57. These results suggest that the synergistic integration of graph attention mechanisms and transfer learning leads to a more robust feature generalization across domains, thereby validating the efficacy of the proposed architecture in leveraging previously learned representations to improve performance on the target ASD classification task.

5.6 Computational Cost

The training fold results demonstrate that the model, with approximately 359K parameters, gradually converged over 166 epochs, requiring a considerable number of iterations before achieving stable generalization. While the early epochs (120) show fluctuating training and validation performance with relatively low loss values and modest accuracy ($\approx 0.71 - 0.74$), consistent improvements emerge only after extended training, with accuracy surpassing 0.70 beyond epoch 60 and reaching a peak test accuracy of 0.76 around epoch 129.

Chapter 6

Conclusion

6.1 Summary

In this paper, a multi-branch Enhanced Graph Convolutional Network (EGCN) that combines Chebyshev spectral graph convolutions with graph attention mechanisms is used to give a novel and effective graph-based deep learning framework for the categorization of Autism Spectrum Disorder. The model may learn rich, complementary feature representations while maintaining the relational structure of the subject population through a site-based population graph by integrating multi-modal inputs such as resting-state functional MRI, structural MRI (sMRI), and phenotypic data. Experimental results on the ABIDE I dataset show that the proposed model outperforms several current baselines, such as autoencoder-based DNNs, state-of-the-art multi-modal deep learning models, and traditional GCNs, with an AUC of 0.82 and a superior classification accuracy of 74.81%. This demonstrates the usefulness of integrating spectral graph learning with attention-based processes for increased discriminative capabilities in neuro-developmental disease categorization.

The contributions of this study are diverse. First, the model architecture presents a systematic means of addressing modality-specific feature extraction using parallel ChebConv branches, followed by late fusion and attention-guided refinement. Second, the usage of a population graph based on acquisition site information provides a scalable and generalizable framework for modeling inter-subject interactions, especially in diverse datasets. Third, detailed ablation studies empirically support the separate contributions of the graph attention layer and hyperparameter optimization, showing the relevance of both structural and

parametric improvements in deep graph models. The implementation of strong assessment procedures, including stratified five-fold cross-validation and ensemble predictions, significantly strengthens the dependability of the reported findings.

6.2 Limitations

A building potential limitation of this study is the lack of experimentation based on site-level cross-validation. The ABIDE I dataset aggregates imaging and phenotypic data from 17 international sites, each characterized by variations in scanner hardware, acquisition protocols, and demographic distributions. These inter-site differences introduce a domain shift that may influence model performance and generalizability. While the proposed multi-branch Graph Convolutional Network (GCN) incorporating Chebyshev Spectral Graph Convolutions, Graph Attention Networks (GATs), and transfer learning techniques demonstrates promising results, all evaluations were conducted without explicitly partitioning data by acquisition site. Consequently, the reported performance metrics may partially reflect site-specific biases rather than true cross-site robustness.

Another important limitation of this study concerns its clinical validity. While the proposed multi-branch Graph Convolutional Network (GCN) with Chebyshev Spectral Graph Convolutions, Graph Attention Networks (GATs), and transfer learning techniques achieves strong performance on the ABIDE I dataset, the findings remain primarily constrained to a research setting. The dataset is composed of retrospective data collected under controlled experimental conditions, and it may not fully capture the variability, comorbidities, and diagnostic complexities encountered in real-world clinical practice. Furthermore, the diagnostic labels in ABIDE I are derived from site-specific clinical assessments, which may lack the uniformity and standardized rigor required for large-scale clinical application.

A notable limitation of the ABIDE I dataset is the imbalance in gender distribution, with a disproportionately higher representation of male participants compared to females. This skew reflects the higher prevalence of Autism Spectrum Disorder (ASD) diagnoses in males but also introduces potential biases in statistical modeling. In traditional machine learning frameworks, such imbalance can inadvertently bias classifiers toward patterns predominantly representative of the male population, thereby reducing generalizability and potentially underestimating ASD-related features present in females. This issue raises concerns regarding the robustness and fairness of models trained on ABIDE I when applied to more balanced or

female-enriched cohorts.

Although, several hyper-parameter tuning was done for the proposed multi-branch GCN, there was no experimentation done with that for the attention layer deployed in the architecture. As the attention layer contributes heavily to the potential achievements in the models performance as shown in Tables 5.1, 5.2, thus, there might be more from the attention layer to offer.

6.3 Future Work

Looking ahead, there are various viable paths to broaden the breadth and effect of this study. Future studies might examine combining new data modalities, such as genetic or behavioral video data, to further improve the models knowledge of ASD heterogeneity. Moreover, adaptive or learnable graph-building approaches may provide more dynamic and data-driven connection modeling between individuals, moving beyond fixed site-based similarity. The generality of the model over diverse datasets, such as ABIDE II or other neuro-developmental cohorts, would be a critical step toward clinical translation. Finally, adding interpretability frameworks into the model may yield neurobiologically significant insights, supporting physicians in identifying crucial biomarkers and processes causing ASD. Overall, this work offers a solid basis for the continuing improvement of graph-based multimodal learning in computational neuropsychiatry.

References

[1] S. Q. Abbas, L. Chi, and Y.-P. P. Chen, "Deepmnf: Deep multimodal neuroimaging framework for diagnosing autism spectrum disorder", *Artificial Intelligence in Medicine*, vol. 136, p. 102 475, 2023.

[2] S. Q. Abbas, L. Chi, and Y.-P. P. Chen, "Deepmnf: Deep multimodal neuroimaging framework for diagnosing autism spectrum disorder", *Artificial Intelligence in Medicine*, vol. 136, p. 102 475, Feb. 2023, ISSN: 09333657. DOI: 10 . 1016 / j . artmed . 2022 . 102475. [Online]. Available: https://linkinghub.elsevier.com/retrieve/pii/S0933365722002275.

[3] A. Abraham, M. P. Milham, A. Di Martino, *et al.*, "Deriving reproducible biomarkers from multi-site resting-state data: An autism-based example", *NeuroImage*, vol. 147, pp. 736–745, 2017.

[4] F. Almuqhim and F. Saeed, "Asd-saenet: A sparse autoencoder, and deep-neural network model for detecting autism spectrum disorder (asd) using fmri data", *Frontiers in Computational Neuroscience*, vol. 15, p. 654 315, 2021.

[5] J. Ashburner, "A fast diffeomorphic image registration algorithm", *Neuroimage*, vol. 38, no. 1, pp. 95–113, 2007.

[6] R. O. Bahado-Singh, S. Vishweswaraiah, B. Aydas, *et al.*, "Artificial intelligence analysis of newborn leucocyte epigenomic markers for the prediction of autism", *Brain research*, vol. 1724, p. 146 457, 2019.

[7] J. Bathelt, J. Holmes, D. E. Astle, *et al.*, "Data-driven subtyping of executive function–related behavioral problems in children", *Journal of the American Academy of Child & Adolescent Psychiatry*, vol. 57, no. 4, pp. 252–262, 2018.

[8] M. A. Bayram,. Özer, and F. Temurta, "Deep learning methods for autism spectrum disorder diagnosis based on fmri images", *Sakarya university journal of computer and information sciences*, vol. 4, no. 1, pp. 142–155, 2021.

[9] C. Cameron, B. Yassine, C. Carlton, *et al.*, "The neuro bureau preprocessing initiative: Open sharing of preprocessed neuroimaging data and derivatives",

Frontiers in Neuroinformatics, vol. 7, 2013. DOI: 10.3389/CONF.FNINF.2013.09.00041/EVENT_ABSTRACT.

[10] F. Campo, A. Retico, S. Calderoni, and P. Oliva, "Multi-site mri data harmonization with an adversarial learning approach: Implementation to the study of brain connectivity in autism spectrum disorders", *Applied Sciences*, vol. 13, no. 11, p. 6486, 2023.

[11] C. Chang and G. H. Glover, "Time–frequency dynamics of resting-state brain connectivity measured with fmri", *Neuroimage*, vol. 50, no. 1, pp. 81–98, 2010.

[12] C. Chlebowski, J. A. Green, M. L. Barton, and D. Fein, "Using the childhood autism rating scale to diagnose autism spectrum disorders", *Journal of autism and developmental disorders*, vol. 40, p. 787, 7 Jul. 2010, ISSN: 01623257. DOI: 10.1007/S10803-009-0926-X. [Online]. Available: https://pmc.ncbi.nlm.nih.gov/articles/PMC3612531/.

[13] A. M. Daniels and D. S. Mandell, "Explaining differences in age at autism spectrum disorder diagnosis: A critical review", *Autism : the international journal of research and practice*, vol. 18, pp. 583–597, 5 2014, ISSN: 1461-7005. DOI: 10.1177/1362361313480277. [Online]. Available: https://pubmed.ncbi.nlm.nih.gov/23787411/.

[14] M. Defferrard, X. Bresson, and P. Vandergheynst, "Convolutional neural networks on graphs with fast localized spectral filtering", *Advances in neural information processing systems*, vol. 29, 2016.

[15] Y. Dong, D. Batalle, and M. Deprez, "A framework for comparison and interpretation of machine learning classifiers to predict autism on the abide dataset", *Human brain mapping*, vol. 46, 5 Apr. 2025, ISSN: 1097-0193. DOI: 10.1002/HBM.70190. [Online]. Available: https://pubmed.ncbi.nlm.nih.gov/40095417/.

[16] F. Doshi-Velez and B. Kim, "Towards a rigorous science of interpretable machine learning", *arXiv preprint arXiv:1702.08608*, 2017.

[17] J. Du, S. Wang, R. Chen, and S. Wang, "Improving fmri-based autism severity identification via brain network distance and adaptive label distribution learning", *IEEE Transactions on Neural Systems and Rehabilitation Engineering*, vol. 33, pp. 162–174, 2025. DOI: 10.1109/TNSRE.2024.3516216.

[18] Y. Du, X. He, P. Kochunov, *et al.*, "A new multimodality fusion classification approach to explore the uniqueness of schizophrenia and autism spectrum disorder", *Human Brain Mapping*, vol. 43, pp. 3887–3903, 12 Aug. 2022, ISSN: 1097-0193. DOI: 10.1002/HBM.25890. [Online]. Available: https://onlinelibrary.wiley.com/doi/full/10.1002/hbm.25890.

[19] C. Ecker, S. Y. Bookheimer, and D. G. Murphy, "Neuroimaging in autism spectrum disorder: Brain structure and function across the lifespan", *The Lancet Neurology*, vol. 14, no. 11, pp. 1121–1134, 2015.

[20] F. EDITION, "Diagnostic and statistical manual of mental disorders", *American Psychiatric Association, Washington, DC*, pp. 205–224, 1980.

[21] F. Edition *et al.*, "Diagnostic and statistical manual of mental disorders", *Am Psychiatric Assoc*, vol. 21, no. 21, pp. 591–643, 2013.

[22] B. Fischl, "Freesurfer", *Neuroimage*, vol. 62, no. 2, pp. 774–781, 2012.

[23] A. El-Gazzar, M. Quaak, L. Cerliani, P. Bloem, G. van Wingen, and R. Mani Thomas, "A hybrid 3dcnn and 3dc-lstm based model for 4d spatio-temporal fmri data: An abide autism classification study", in *International Workshop on OR 2.0 Context-Aware Operating Theaters*, Springer, 2019, pp. 95–102.

[24] K. Gupta, A. Aly, and E. Ifeachor, "Cross-domain transfer learning for domain adaptation in autism spectrum disorder diagnosis", in *18th International Conference on Health Informatics*, 2025.

[25] J. Gutiérrez, Z. Che, G. Zhai, and P. Le Callet, "Saliency4asd: Challenge, dataset and tools for visual attention modeling for autism spectrum disorder", *Signal Processing: Image Communication*, vol. 92, p. 116 092, 2021.

[26] J. Hashemi, G. Dawson, K. L. Carpenter, *et al.*, "Computer vision analysis for quantification of autism risk behaviors", *IEEE Transactions on Affective Computing*, vol. 12, no. 1, pp. 215–226, 2018.

[27] M. He, Z. Wei, and J.-R. Wen, "Convolutional neural networks on graphs with chebyshev approximation, revisited", *Advances in neural information processing systems*, vol. 35, pp. 7264–7276, 2022.

[28] M. He, Z. Wei, H. Xu, *et al.*, "Bernnet: Learning arbitrary graph spectral filters via bernstein approximation", *Advances in neural information processing systems*, vol. 34, pp. 14 239–14 251, 2021.

[29] A. S. Heinsfeld, A. R. Franco, R. C. Craddock, A. Buchweitz, and F. Meneguzzi, "Identification of autism spectrum disorder using deep learning and the abide dataset", *NeuroImage: Clinical*, vol. 17, pp. 16–23, 2018, ISSN: 22131582. DOI: 10.1016/j.nicl.2017.08.017.

[30] S.-J. Hong, S. L. Valk, A. Di Martino, M. P. Milham, and B. C. Bernhardt, "Multidimensional neuroanatomical subtyping of autism spectrum disorder", *Cerebral Cortex*, vol. 28, no. 10, pp. 3578–3588, 2018.

[31] Y. Huang and A. C. Chung, "Edge-variational graph convolutional networks for uncertainty-aware disease prediction", in *Medical Image Computing and Computer Assisted Intervention–MICCAI 2020: 23rd International Conference, Lima, Peru, October 4–8, 2020, Proceedings, Part VII 23*, Springer, 2020, pp. 562–572.

[32] V. Jain, C. T. Rakshe, S. S. Sengar, M. Murugappan, and J. F. A. Ronickom, "Age-and severity-specific deep learning models for autism spectrum disorder classification using functional connectivity measures", *Arabian Journal for Science and Engineering*, vol. 49, no. 5, pp. 6847–6865, 2024.

[33] N. A. Khan and X. Shang, "Asd-gannet: A generative adversarial network-inspired deep learning approach for the classification of autism brain disorder", *Brain Sciences*, vol. 14, no. 8, p. 766, 2024.

[34] M. Khosla, K. Jamison, A. Kuceyeski, and M. R. Sabuncu, "3d convolutional neural networks for classification of functional connectomes", in *international workshop on deep learning in medical image analysis*, Springer, 2018, pp. 137–145.

[35] L. Li, H. Jiang, G. Wen, *et al.*, "Te-hi-gcn: An ensemble of transfer hierarchical graph convolutional networks for disorder diagnosis", *Neuroinformatics*, vol. 20, pp. 353–375, 2 Apr. 2022, ISSN: 15590089. DOI: 10.1007/S12021-021-09548-1/METRICS. [Online]. Available: https://link.springer.com/article/10.1007/s12021-021-09548-1.

[36] M. V. Lombardo, M.-C. Lai, and S. Baron-Cohen, "Big data approaches to decomposing heterogeneity across the autism spectrum", *Molecular psychiatry*, vol. 24, no. 10, pp. 1435–1450, 2019.

[37] C. Lord, T. S. Brugha, T. Charman, *et al.*, "Autism spectrum disorder", *Nature reviews. Disease primers*, vol. 6, 1 Jan. 2020, ISSN: 2056-676X. DOI: 10.1038/S41572-019-0138-4. [Online]. Available: https://pubmed.ncbi.nlm.nih.gov/31949163/.

[38] C. Lord, T. Charman, A. Havdahl, *et al.*, "The lancet commission on the future of care and clinical research in autism", *The Lancet*, vol. 399, no. 10321, pp. 271–334, 2022.

[39] C. Lord, M. Rutter, S. Goode, *et al.*, "Autism diagnostic observation schedule: A standardized observation of communicative and social behavior", *Journal of autism and developmental disorders*, vol. 19, pp. 185–212, 2 Jun. 1989, ISSN: 0162-3257. DOI: 10.1007/BF02211841. [Online]. Available: https://pubmed.ncbi.nlm.nih.gov/2745388/.

[40] C. Lord, M. Rutter, and A. Le Couteur, "Autism diagnostic interview-revised: A revised version of a diagnostic interview for caregivers of individuals with possible pervasive developmental disorders", *Journal of autism and developmental disorders*, vol. 24, no. 5, pp. 659–685, 1994.

[41] Y. Ma, X. Mu, T. Zhang, and Y. Zhao, "Maft-so: A novel multi-atlas fusion template based on spatial overlap for asd diagnosis", *Journal of Biomedical Informatics*, vol. 157, p. 104 714, Sep. 2024, ISSN: 1532-0464. DOI: 10.1016/J.JBI.2024.104714.

[42] M. J. Maenner, K. A. Shaw, A. V. Bakian, *et al.*, "Prevalence of autism spectrum disorder among children aged 8 yearsautism and developmental disabilities monitoring network, 11 sites, united states, 2020", *MMWR Surveillance Summaries*, vol. 72, no. 2, p. 1, 2023.

[43] S. Majumder, F. Apicella, F. Muratori, and K. Das, "Detecting autism spectrum disorder using topological data analysis", in *ICASSP 2020-2020 IEEE International Conference on Acoustics, Speech and Signal Processing (ICASSP)*, IEEE, 2020, pp. 1210–1214.

[44] A. D. Martino, C. G. Yan, Q. Li, *et al.*, "The autism brain imaging data exchange: Towards a large-scale evaluation of the intrinsic brain architecture in autism", *Molecular Psychiatry 2014 19:6*, vol. 19, pp. 659–667, 6 Jun. 2013, ISSN: 1476-5578. DOI: 10.1038/mp.2013.78. [Online]. Available: https://www.nature.com/articles/mp201378.

[45] A. M. Pagnozzi, E. Conti, S. Calderoni, J. Fripp, and S. E. Rose, "A systematic review of structural mri biomarkers in autism spectrum disorder: A machine learning perspective", *International Journal of Developmental Neuroscience*, vol. 71, pp. 68–82, 2018.

[46] S. J. Pan and Q. Yang, "A survey on transfer learning", *IEEE Transactions on knowledge and data engineering*, vol. 22, no. 10, pp. 1345–1359, 2009.

[47] S. Parisot, S. I. Ktena, E. Ferrante, *et al.*, "Disease prediction using graph convolutional networks: Application to autism spectrum disorder and alzheimers disease", *Medical image analysis*, vol. 48, pp. 117–130, 2018.

[48] S. Rajaprakash, C. B. Basha, C. S. Ram, I. Ameethbasha, V. Subapriya, and R. Sofia, "Using convolutional network in graphical model detection of autism disorders with fuzzy inference systems", *Intelligence-Based Medicine*, vol. 11, p. 100 213, 2025, ISSN: 26665212. DOI: 10.1016/j.ibmed.2025.100213.

[49] M. Raki, M. Cabezas, K. Kushibar, A. Oliver, and X. Lladó, "Improving the detection of autism spectrum disorder by combining structural and functional mri information", *NeuroImage: Clinical*, vol. 25, p. 102 181, 2020.

[50] A. Rathore, S. Palande, J. S. Anderson, B. A. Zielinski, P. T. Fletcher, and B. Wang, "Autism classification using topological features and deep learning: A cautionary tale", in *International Conference on Medical Image Computing and Computer-Assisted Intervention*, Springer, 2019, pp. 736–744.

[51] J. Rehg, G. Abowd, A. Rozga, *et al.*, "Decoding children's social behavior", in *Proceedings of the IEEE conference on computer vision and pattern recognition*, 2013, pp. 3414–3421.

[52] K. Riddle, C. J. Cascio, and N. D. Woodward, "Brain structure in autism: A voxel-based morphometry analysis of the autism brain imaging database exchange (abide)", *Brain imaging and behavior*, vol. 11, no. 2, pp. 541–551, 2017.

[53] G. Riva and E. Riva, "De-enigma: Multimodal human–robot interaction for teaching and expanding social imagination in autistic children.", *CyberPsychology, Behavior & Social Networking*, vol. 23, no. 11, 2020.

[54] S. Saponaro, A. Giuliano, R. Bellotti, *et al.*, "Multi-site harmonization of mri data uncovers machine-learning discrimination capability in barely separable populations: An example from the abide dataset", *NeuroImage: Clinical*, vol. 35, p. 103 082, 2022.

[55] S. Saponaro, F. Lizzi, G. Serra, *et al.*, "Deep learning based joint fusion approach to exploit anatomical and functional brain information in autism spectrum disorders", *Brain Informatics*, vol. 11, pp. 1–13, 1 Dec. 2024, ISSN: 21984026. DOI: 10.1186/S40708-023-00217-4/FIGURES/4. [Online]. Available: https://link.springer.com/articles/10.1186/s40708-023-00217-4.

[56] I. Shahzad, S. U. R. Khan, A. Waseem, Z. U. Abideen, and J. Liu, "Enhancing asd classification through hybrid attention-based learning of facial features", *Signal, Image and Video Processing*, vol. 18, no. Suppl 1, pp. 475–488, 2024.

[57] K. A. Shaw, "Prevalence and early identification of autism spectrum disorder among children aged 4 and 8 yearsautism and developmental disabilities monitoring network, 16 sites, united states, 2022", *MMWR. Surveillance Summaries*, vol. 74, 2025.

[58] S. Shrivastava, U. Mishra, N. Singh, A. Chandra, and S. Verma, "Control or autism-classification using convolutional neural networks on functional mri", in *2020 11th International Conference on Computing, Communication and Networking Technologies (ICCCNT)*, IEEE, 2020, pp. 1–6.

[59] T. Song, Z. Ren, J. Zhang, and M. Wang, "Multi-view and multimodal graph convolutional neural network for autism spectrum disorder diagnosis",

Mathematics 2024, Vol. 12, Page 1648, vol. 12, p. 1648, 11 May 2024, ISSN: 2227-7390. DOI: 10 . 3390 / MATH12111648. [Online]. Available: https://www.mdpi.com/2227-7390/12/11/1648.

[60] J. Stember, D. Stember, L. Pasquini, J. Merhnaz, A. Holodny, and H. Shalu, "Deep reinforcement learning for fmri prediction of autism spectrum disorder", *arXiv preprint arXiv:2206.11224*, 2022.

[61] K. A. Stigler, B. C. McDonald, A. Anand, A. J. Saykin, and C. J. McDougle, "Structural and functional magnetic resonance imaging of autism spectrum disorders", *Brain research*, vol. 1380, pp. 146–161, Mar. 2011, ISSN: 1872-6240. DOI: 10 . 1016 / J . BRAINRES . 2010 . 11 . 076. [Online]. Available: https://pubmed.ncbi.nlm.nih.gov/21130750/.

[62] Y. Tao and M.-L. Shyu, "Sp-asdnet: Cnn-lstm based asd classification model using observer scanpaths", in *2019 IEEE International conference on multimedia & expo workshops (ICMEW)*, IEEE, 2019, pp. 641–646.

[63] P. M. Thompson, E. R. Sowell, N. Gogtay, *et al.*, "Structural mri and brain development", *International review of neurobiology*, vol. 67, pp. 285–323, 2005.

[64] T. Tommasi, F. Orabona, and B. Caputo, "Safety in numbers: Learning categories from few examples with multi model knowledge transfer", in *2010 IEEE Computer Society Conference on Computer Vision and Pattern Recognition*, IEEE, 2010, pp. 3081–3088.

[65] B. G. Travers, N. Adluru, C. Ennis, *et al.*, "Diffusion tensor imaging in autism spectrum disorder: A review", *Autism Research*, vol. 5, no. 5, pp. 289–313, 2012.

[66] L. Q. Uddin, K. Supekar, and V. Menon, "Reconceptualizing functional brain connectivity in autism from a developmental perspective", *Frontiers in human neuroscience*, vol. 7, p. 458, 2013.

[67] G. Varoquaux, "Cross-validation failure: Small sample sizes lead to large error bars", *NeuroImage*, vol. 180, pp. 68–77, 2018.

[68] P. Velikovi, G. Cucurull, A. Casanova, A. Romero, P. Lio, and Y. Bengio, "Graph attention networks", *arXiv preprint arXiv:1710.10903*, 2017.

[69] M. Wang, J. Guo, Y. Wang, M. Yu, and J. Guo, "Multimodal autism spectrum disorder diagnosis method based on deepgcn", *IEEE Transactions on Neural Systems and Rehabilitation Engineering*, vol. 31, pp. 3664–3674, 2023, ISSN: 15580210. DOI: 10.1109/TNSRE.2023.3314516.

[70] Z. Wang, Y. Xu, D. Peng, J. Gao, and F. Lu, "Brain functional activity-based classification of autism spectrum disorder using an attention-based graph

neural network combined with gene expression", *Cerebral Cortex*, vol. 33, no. 10, pp. 6407–6419, 2023.

[71] I. H. Witten and E. Frank, "Data mining: Practical machine learning tools and techniques with java implementations", *Acm Sigmod Record*, vol. 31, no. 1, pp. 76–77, 2002.

[72] W. Yan, G. Qu, W. Hu, *et al.*, "Deep learning in neuroimaging: Promises and challenges", *IEEE Signal Processing Magazine*, vol. 39, no. 2, pp. 87–98, 2022.

[73] B. Yu, H. Yin, and Z. Zhu, "Spatio-temporal graph convolutional networks: A deep learning framework for traffic forecasting", *arXiv preprint arXiv:1709.04875*, 2017.

[74] R. Zhang, F. Sheng, L. Wang, and W. Zeng, "Research on multi-center assisted diagnosis of asd based on multimodal feature fusion", *International Journal of Imaging Systems and Technology*, vol. 34, no. 3, e23110, 2024. DOI: https://doi.org/10.1002/ima.23110. [Online]. Available: https://onlinelibrary.wiley.com/doi/abs/10.1002/ima.23110.

[75] R. Zhang, F. Sheng, L. Wang, and W. Zeng, "Research on multi-center assisted diagnosis of asd based on multimodal feature fusion", *International Journal of Imaging Systems and Technology*, vol. 34, e23110, 3 May 2024, ISSN: 1098-1098. DOI: 10.1002/IMA.23110. [Online]. Available: https://onlinelibrary.wiley.com/doi/full/10.1002/ima.23110.

[76] S. Zhang, H. Tong, J. Xu, and R. Maciejewski, "Graph convolutional networks: A comprehensive review", *Computational Social Networks*, vol. 6, no. 1, pp. 1–23, 2019.

[77] A. Zia, A. Khamis, J. Nichols, *et al.*, "Topological deep learning: A review of an emerging paradigm", *Artificial Intelligence Review*, vol. 57, no. 4, p. 77, 2024.

[78] A. Zunino, P. Morerio, A. Cavallo, *et al.*, "Video gesture analysis for autism spectrum disorder detection", in *2018 24th International Conference on Pattern Recognition (ICPR)*, 2018, pp. 3421–3426. DOI: 10.1109/ICPR.2018.8545095.

[79] L. Zwaigenbaum, M. L. Bauman, W. L. Stone, *et al.*, "Early identification of autism spectrum disorder: Recommendations for practice and research", *Pediatrics*, vol. 136 Suppl 1, S10–S40, Suppl 1 Oct. 2015, ISSN: 1098-4275. DOI: 10.1542/PEDS.2014-3667C. [Online]. Available: https://pubmed.ncbi.nlm.nih.gov/26430168/.

List of Publications

1. Adnan Ferdous Ashrafi and Md. Hasanul Kabir, '**An enhanced Graph Convolutional Network using Chebyshev Spectral Graph and Graph Attention for Autism Spectrum Disorder Classification**," Accepted for publication at 6^{th} *International Conference on Electrical, Communication and Computer Engineering (ICECCE)*, Istanbul, Turkey, August 27-28, 2025.